Imaging Manifestations of the Leukodystrophies, Inherited Disorders of White Matter

Edward Yang, MD, PhD*,
Sanjay P. Prabhu, MBBS, MRCPCH, FRCR

KEYWORDS

• Leukodystrophy • Inborn error of metabolism • Dysmyelination • Demyelination • Spectroscopy • White matter

KEY POINTS

- Recognition of leukodystrophies requires a solid understanding of normal myelination.
- When a leukodystrophy is encountered, a pattern-based approach is useful for developing a reasonably sized differential diagnosis. The patterns stressed in this review include globally delayed myelination, subcortical white matter predominant, central white matter predominant, and combined gray/white matter patterns.
- Special emphasis should be placed on recognizing unusual combinations of findings that suggest a specific diagnosis.

INTRODUCTION

In contrast to most other white matter diseases discussed in this issue, leukodystrophies are inherited disorders that result from mutations in a specific gene product or biological pathway. Various working definitions of leukodystrophy have been proposed that further restrict the meaning of this term to inborn errors of metabolism (ie, a specific type of gene product) or demyelination (ie, a specific pathogenic mechanism).[1–3] Matters become more complicated still because some investigators define demyelination as any process leading to myelin loss, whereas some would restrict the meaning of this term to inflammatory disorders such as multiple sclerosis, leaving disorders of myelin synthesis/maintenance under the grouping of 'dysmyelination.'

Because there is considerable overlap in the appearance of inherited white matter diseases regardless of type of gene product or pathogenesis of the signal abnormality seen on imaging, this review uses a pragmatic definition of leukodystrophy, namely any disorder of white matter signal secondary to a defective or absent gene product. Although this definition is fairly broad, it excludes disorders that exclusively affect gray matter structures or at least lack discrete white matter signal abnormality. Therefore, this article excludes some well-known metabolic disorders such as pantothenate kinase deficiency, creatine deficiency syndromes, and many of the organic acidemias (eg, 3-methylgluconic and methylmalonic acidemia). Diffuse white matter disease seen in association with congenital muscular dystrophies has a distinctive clinical presentation,[4–6] and imaging of disorders of peroxisomal biogenesis have been recently reviewed elsewhere[7]; both are also omitted from this review.

As a category, the leukodystrophies usually present a challenge to radiologists because specific disease entities are rarely encountered and there are numerous diseases with overlapping imaging appearance. In this review, a practical approach

Department of Radiology, Boston Children's Hospital, Harvard Medical School, 300 Longwood Avenue, Boston, MA 02115, USA
* Corresponding author. Department of Radiology, Boston Children's Hospital, 300 Longwood Avenue, Boston, MA 02115.
E-mail address: edward.yang@childrens.harvard.edu

Radiol Clin N Am 52 (2014) 279–319
http://dx.doi.org/10.1016/j.rcl.2013.11.008
0033-8389/14/$ – see front matter

to recognizing and categorizing the leukodystrophies is described, focusing on 4 common patterns of signal abnormality in the brain parenchyma (**Box 1**). Special emphasis is given to unusual imaging features or combinations of features that suggest a specific diagnosis. For the interested reader, additional resources are provided, including reference works dedicated to the topic.[8–10]

IMAGE ACQUISITION

As with other white matter disorders, leukodystrophies are best appreciated on magnetic resonance (MR) imaging.[11] Standard MR imaging protocols should include high-resolution T1-weighted and T2-weighted imaging in at least 2 planes to provide an accurate evaluation of the maturity and integrity of brain myelination. Diffusion-weighted imaging is

Box 1
Simplified pattern-based approach to leukodystrophies

Globally Arrested/Absent Myelination

Pelizaeus-Merzbacher disease
18q-deletion syndrome
Free sialic acid storage disorders (Salla)
Trichothiodystrophy
Cockayne syndrome*
Fucosidosis
Hypomyelination with hypodontia and hypogonadotropic hypogonadism (4H syndrome)
Hypomyelination with atrophy of the basal ganglia and cerebellum*
Hypomyelination with congenital cataracts
Nonketotic hyperglycinemia

Subcortical Predominant White Matter Signal Abnormality

Galactosemia
Megalencephalic leukoencephalopathy with subcortical cysts*
Aicardi-Goutières syndrome*

Central White Matter Predominant Signal Abnormality, With or Without Brainstem Involvement

X-linked adrenoleukodystrophy, acyl-coenzyme A oxidase deficiency*
Metachromatic leukodystrophy
Mucopolysaccharidosis
Lowe syndrome*
X-linked Charcot-Marie-Tooth*
Cockayne syndrome+
Vanishing white matter disease (childhood ataxia with central nervous system hypomyelination)
Neuronal ceroid lipofuscinosis+
Leukoencephalopathy with brainstem and spinal cord evolvement and increased lactate*
Phenylketonuria
Sjögren-Larsson syndrome
Nonketotic hyperglycinemia
Hyperhomocysteinemia
Biotinidase (multiple carboxylase) deficiency

Combination of Gray and White Matter Signal Abnormality

Canavan disease*
GM1/GM2 gangliosidoses (Tay-Sachs, Sandhoff syndromes)*
Alexander disease*
Krabbe disease*
Maple syrup urine disease*
Leigh disease and other mitochondrial disorders
Urea cycle disorders*
L-2-hydroxyglutaric aciduria*
Glutaric aciduria type I and II

* indicates a disease with highly characteristic imaging findings.
+ indicates a minority manifestation.
Data from Barkovich AJ, Patay Z. Metabolic, toxic, and inflammatory brain disorders. In: Barkovich AJ, editor. Pediatric neuroimaging. Philadelphia: Lippincott Williams & Wilkins; 2012. p. 81–239.

also essential because it often shows parenchymal changes to greatest advantage,[12] particularly in the setting of acute clinical deterioration (**Box 2**). For detection of mineralization (ie, calcium, iron), susceptibility-weighted imaging can increase conspicuity on MR imaging. Gadolinium-based contrast is frequently omitted for workups where a leukodystrophy is a possibility (eg, developmental delay). However, gadolinium-based contrast medium can increase the specificity of the diagnosis because enhancement is a prominent feature in several leukodystrophies (**Box 3**), and this enhancement can be used to follow disease activity in some disorders (eg, X-linked adrenoleukodystrophy [ALD]).[13] MR spectroscopy is also helpful in building evidence for a metabolic disturbance (ie, lactate)[14,15] and in some cases can suggest a specific diagnosis (**Box 4**). Two important caveats apply with MR spectroscopy. First, some lactate within the cerebrospinal fluid (CSF) is normal in the first few months of life, and therefore, exclusion of CSF in the interrogated voxel is important for avoiding false-positives. Second, there is evidence that the inverted lactate doublet seen images with intermediate echo time (TE) = 144 millisecond is attenuated at 3 T, and therefore adding a 288-ms acquisition should be considered to avoid this effect.[16]

APPROACH TO IMAGE INTERPRETATION

Recognition that there is an abnormality of white matter is the first obvious step in accurately diagnosing a leukodystrophy. This recognition is more difficult than it might first appear because the patients presenting for leukodystrophy evaluation are usually at an age where immature/incomplete brain myelination is expected. Also, leukodystrophies tend to present in a left-right symmetric fashion similar to immature myelination

Box 2
Leukodystrophies featuring restricted diffusion

Leigh disease, mitochondrial disorder

Maple syrup urine disorder

Urea cycle disorders

Canavan

Metachromatic leukodystrophy

Hyperhomocysteinemia

X-linked adrenoleukodystrophy

Nonketotic hyperglycemia

Leukoencephalopathy with brainstem and spinal cord evolvement and increased lactate

Vanishing white matter disease

Data from Barkovich AJ, Patay Z. Metabolic, toxic, and inflammatory brain disorders. In: Barkovich AJ, editor. Pediatric neuroimaging. Philadelphia: Lippincott Williams & Wilkins; 2012. p. 81–239, with permission; and Patay Z. Diffusion-weighted MR imaging in leukodystrophies. Eur Radiol 2005;15(11):2284–303.

Box 3
Leukodystrophies with enhancement

Krabbe disease (cranial nerves, cauda equina)

Metachromatic leukodystrophy (cranial nerves, cauda equina)

X-linked adrenoleukodystrophy, acyl-coenzyme A oxidase deficiency

Alexander disease

Box 4
MR spectroscopy findings in leukodystrophies

Unusual MR Spectroscopy Peaks Associated with Specific Disorders

Phenylketonuria (phenylanaline 7.37 ppm)
Maple syrup urine disease (branched-chain amino acids/ketoacids, 0.9 ppm)
Salla/Canavan disease (increased *N*-acetylaspartate)
Sjögren-Larsson (0.9 and 1.3 ppm peaks that do no suppress with long echo time)
Creatinine deficiency syndromes (decreased creatinine)
Succinate dehydrogenase (Leigh syndrome: 2.4 ppm succinate peak)
Fucosidosis (1.2 ppm doublet, 3.4–3.8 ppm broad peak)
Galactosemia (galactitol 3.67 and 3.74 ppm)
Nonketotic hyperglycinemia (glycine 3.56 ppm)
Urea cycle disorders (glutamine/glutamate 2.05–2.55 and 3.68–3.85 ppm)

Leukodystrophies Where Lactate Is Commonly Encountered

Mitochondrial disorders
Maple syrup urine disease
Krabbe
Alexander
Zellweger disease
Hyperhomocysteinemia
Biotinidase (multiple carboxylase deficiency)
X-linked adrenoleukodystrophy
Vanishing matter disease

Data from Barkovich AJ, Patay Z. Metabolic, toxic, and inflammatory brain disorders. In: Barkovich AJ, editor. Pediatric neuroimaging. Philadelphia: Lippincott Williams & Wilkins; 2012. p. 81–239.

with some rare exceptions.[17,18] As a result, it is easy to incorrectly dismiss hyperintensity in the white mater as immature myelination rather than pathology. To avoid this pitfall, it is essential that an accurate reference for age-specific myelination patterns is readily available to radiologists who interpret pediatric brain imaging studies (see the article by Guleria and Kelly elsewhere in this issue[19]). Knowledge of normal myelination milestones allows accurate detection of delayed myelination and T2 signal abnormality outside expected sites. Specifically, it allows recognition of both delayed myelination as well as cases where the T2 signal has exceeded that expected for immature myelination alone in a particular location.

Most classification systems for leukodystrophies focus on specific biochemical abnormalities (eg, organic acidemias) or the organelle implicated with a specific leukodystrophy (eg, lysosomal disorder).[3,9] However, the imaging appearances of leukodystrophies categorized in this fashion can vary dramatically, and the practicing radiologist usually is most concerned with imaging features. Therefore, in this article, the leukodystrophies are subdivided by imaging pattern and a simplified version of pattern-based approaches is used as described in more detail elsewhere.[10,20]

The 4 patterns to be discussed are summarized in **Box 1**.

1. Generalized delay or failure in myelination. In these disorders, the myelination has the appearance of a much younger patient and in some cases is entirely absent. The T2 hyperintensity does not typically exceed that seen in brains with immature myelination and lacks focality.
2. Peripheral white matter predominant signal abnormality. Although subcortical white matter is the last to myelinate, disorders in this category feature T2 hyperintensity greater than seen with unmyelinated white matter or focal areas of more pronounced signal increase.
3. Central white matter predominant signal abnormality, with or without brainstem involvement. Here, central white matter is defined as the deep (corona radiata, centrum semiovale) and periventricular white matter. These leukodystrophies tend to spare the subcortical white matter initially and therefore should not be mistaken for globally delayed myelination.
4. Combined gray and white matter signal abnormality. In these disorders, abnormal T2 hyperintensity also affects gray matter structures in either the cortex or deep gray nuclei as well as the white matter.

Within these 4 patterns, particular emphasis should be placed on recognizing disorders with highly characteristic or pathognomonic findings (see asterisks in **Box 1**). The reason is that most of the leukodystrophies are individually rare, representing at most 10% to 20% of all leukodystrophies (population incidence of leukodystrophies are estimated at 1 in 50 to 100,000 live births with 1 report suggesting 1 in 8000).[21–23] As a result, the relative frequency of a specific disorder is a somewhat unreliable guide to pretest probability: it is generally unknown in any given clinical population and the relative incidence of specific disorders is difficult to ascertain confidently outside the most common disorders (eg, Pelizaeus-Merzbacher, metachromatic leukodystrophy, mitochondrial disorders, and adrenoleukodystrophy). Some additional unique (although not necessarily specific) imaging findings are listed in **Box 5**. Of particular interest are anterior-posterior and centrifugal/centripetal gradients in the pattern of white matter involvement, something that can be used to differentiate disorders within 1 of the 4 patterns.

Before discussing these 4 patterns in depth, a few general principles should be kept in mind. First, leukodystrophies are generally progressive, leading to diffuse white matter disease and atrophy. Therefore, even highly characteristic imaging patterns become nonspecific at the end stage of disease (**Figs. 1** and **2**). Second, there is a wide spectrum of severity depending on the degree of functional gene product remaining. As a result, there are usually neonatal, infantile, juvenile, and even adult manifestations of most leukodystrophies. Third, restricted diffusion is a common and helpful finding in patients with leukodystrophy, particularly when imaging is performed during an episode of clinical deterioration. However, these sites of restricted diffusion are not always an indicator of cytotoxic edema and irreversible injury. In many instances, these sites of restricted diffusion actually represent myelin vacuolization[9,12] and may improve with supportive or medical therapy (eg, **Fig. 3**). Fourth, some humility is required when interpreting studies performed as part of a leukodystrophy evaluation. As noted earlier, these disorders are individually rare. This makes statements on typical imaging manifestations for a specific disorder difficult, and the diversity of causative mutations in any particular disorder make sweeping generalizations even more problematic. Ultimately, communication between the referring physician and the radiologist becomes essential in guiding a sensible workup; for example, dermatologic, auditory, ophthalmologic, and head circumference data may be completely unknown to the interpreting radiologist but in many instances provide critical clues to a specific diagnosis (**Box 6**).[24] Similarly, newborn screening results vary widely from state

Box 5
Additional imaging findings in the leukodystrophies

Centripetal White Matter Involvement (Subcortical → Periventricular)

L-2-hydroxyglutaric aciduria
Canavan disease
Urea cycle
Kearns-Sayre

Centrifugal White Matter Involvement (Periventricular → Subcortical)

Krabbe disease
Metachromatic leukodystrophy
X-linked adrenoleukodystrophy
Phenylketonuria
Mucopolysaccharidosis
Vanishing white matter disease

Anterior/Posterior Gradient of White Matter disease

Aicardi- Goutières syndrome (anterior)
Alexander disease (anterior)
L-2-hydroxyglutaric aciduria (anterior)
Megencephalic leukoencephalopathy with subcortical cysts (anterior)
Infantile metachromatic leukodystrophy (posterior)
Krabbe disease (posterior)
X-linked adrenoleukodystrophy (posterior)
Mucopolysaccharidoses (posterior)

Parenchymal Calcifications

Aicardi- Goutières (basal ganglia, thalami, dentate, deep/subcortical white matter)
Cockayne syndrome (basal ganglia, dentate, subcortical white matter)
Krabbe disease
X-linked adrenoleukodystrophy (parietooccipital)
TORCH/human immunodeficiency virus

Central Tegmental Tracts Signal Abnormality

Mitochondrial (respiratory chain) diseases
Menkes disease
Vanishing white matter disease
Nonketotic hyperglycinemia
Maple syrup urine disease
Glutaric aciduria I

Data from Barkovich AJ, Patay Z. Metabolic, toxic, and inflammatory brain disorders. In: Barkovich AJ, editor. Pediatric neuroimaging. Philadelphia: Lippincott Williams & Wilkins; 2012. p. 81–239.

to state (see http://www.babysfirsttest.org/newborn-screening/states),[25] and as a result the referring clinician may already possess informative biochemical data that pertain to an abnormal brain MR imaging.

PATTERN 1: ARRESTED/ABSENT MYELINATION

Pelizaeus-Merzbacher Disease

Pelizaeus-Merzbacher disease (PMD) is the prototypical disease of arrested or absent myelination, featuring symptoms of nystagmus, ataxia, developmental delay (cognitive as well as psychomotor), and hypotonia that progresses to spasticity. Patients with the connatal form of the disease present at birth and typically die in early childhood, whereas patients presenting in infancy (usually by 1 year) are said to have the more common classic form of the disease with life expectancy potentially into middle adulthood.[26] PMD is caused by abnormalities in the proteolipid protein 1 (*PLP1*) gene locus located on the X chromosome (Xq22), explaining the predominance of PMD in male patients. *PLP1* is 1 of the 2 major protein constituents of the myelin coat secreted by oligodendrocytes; the other one is myelin basic protein (MBP).[27] Although intuitively deletions or loss of function mutations in *PLP1* might be expected to lead to myelin synthesis failure directly, the

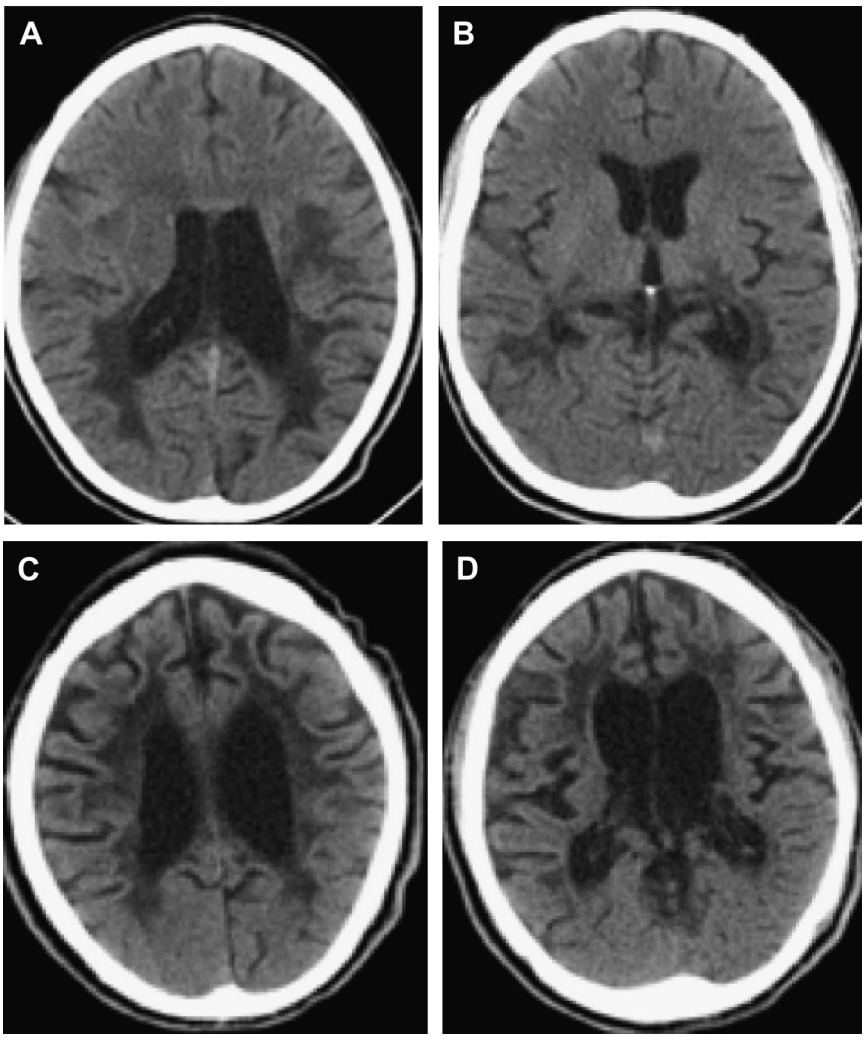

Fig. 1. Progressive white matter changes from X-linked adrenoleukodystrophy at 15 (*A, B*) and 21 (*C, D*) years of age. The classic involvement of the splenium and parietooccipital white matter is obvious on the initial computed tomography study. By the follow-up study, there is nonspecific end-stage white matter disease with volume loss and diffuse hypodensity of the cerebral white matter.

genetics is much more complicated and reflects exquisite sensitivity to gene dosage. Most cases (classic PMD) are caused by duplications of the entire gene locus. Truncating/nonsense mutations or deletions in *PLP1* as well as missense mutations sparing the *PLP1* alternative splicing isoform *DM20* (the embryologically expressed form of *PLP1*) cause mild forms of PMD as well as the related disorder of spastic paraplegia type 2. Missense mutations affecting both *DM20* and *PLP1* lead to the more severe connatal phenotype (hypothesized to reflect an unfolded protein response), as can rare triplications or quintiplication of the *PLP1* locus.[26,28–30] Imaging findings are characterized by absent myelination in the connatal form or arrest of myelination in an early infant pattern for the classic form (**Fig. 4**), the latter associated with some progressive volume loss.[31]

18q Deletion Syndrome

18q deletion syndrome is a somatic chromosome counterpart to PMD, featuring variable dysmorphology (auriculoaural atresia, short stature, midface hypoplasia, extremity deformity) and mental retardation. There is significant phenotypic variability even within pedigrees bearing the same mutation, arguing against simple relationships between specific deletions and phenotype.[32] However, the core phenotypes described earlier seem to best correlate with distal deletions, 18q22.3 through the telomere.[32,33] The fact that

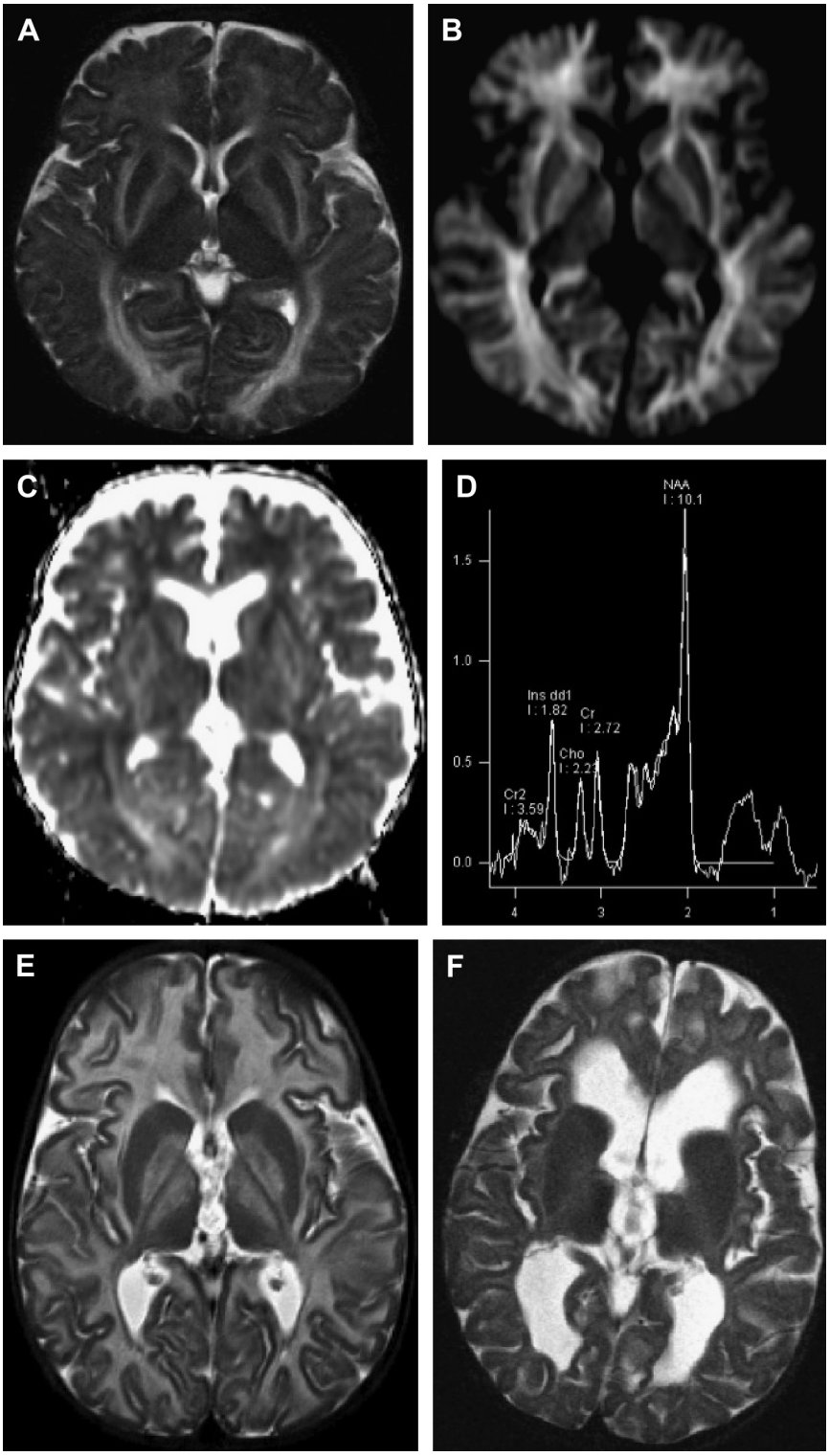

Fig. 2. Eight-month-old with Canavan disease. Axial T2-weighted image (*A*) demonstrates subcortical white matter signal increase greater than expected for immature myelination and signal increase involving the globus pallidus. Apparent diffusion coefficient and diffusion-weighted trace images (*B, C*) demonstrate restricted diffusion in the white matter. MR spectroscopy (*D*) demonstrates marked increase in *N*-acetylaspartate (NAA) relative to choline (Cho), particularly considering patient age. Progressive atrophy of Canavan is demonstrated in another case imaged at 2 years (*E*) and 8 years (*F*) of age. By 8 years of age, there is diffuse white matter atrophy although the globus pallidus signal abnormality has abated.

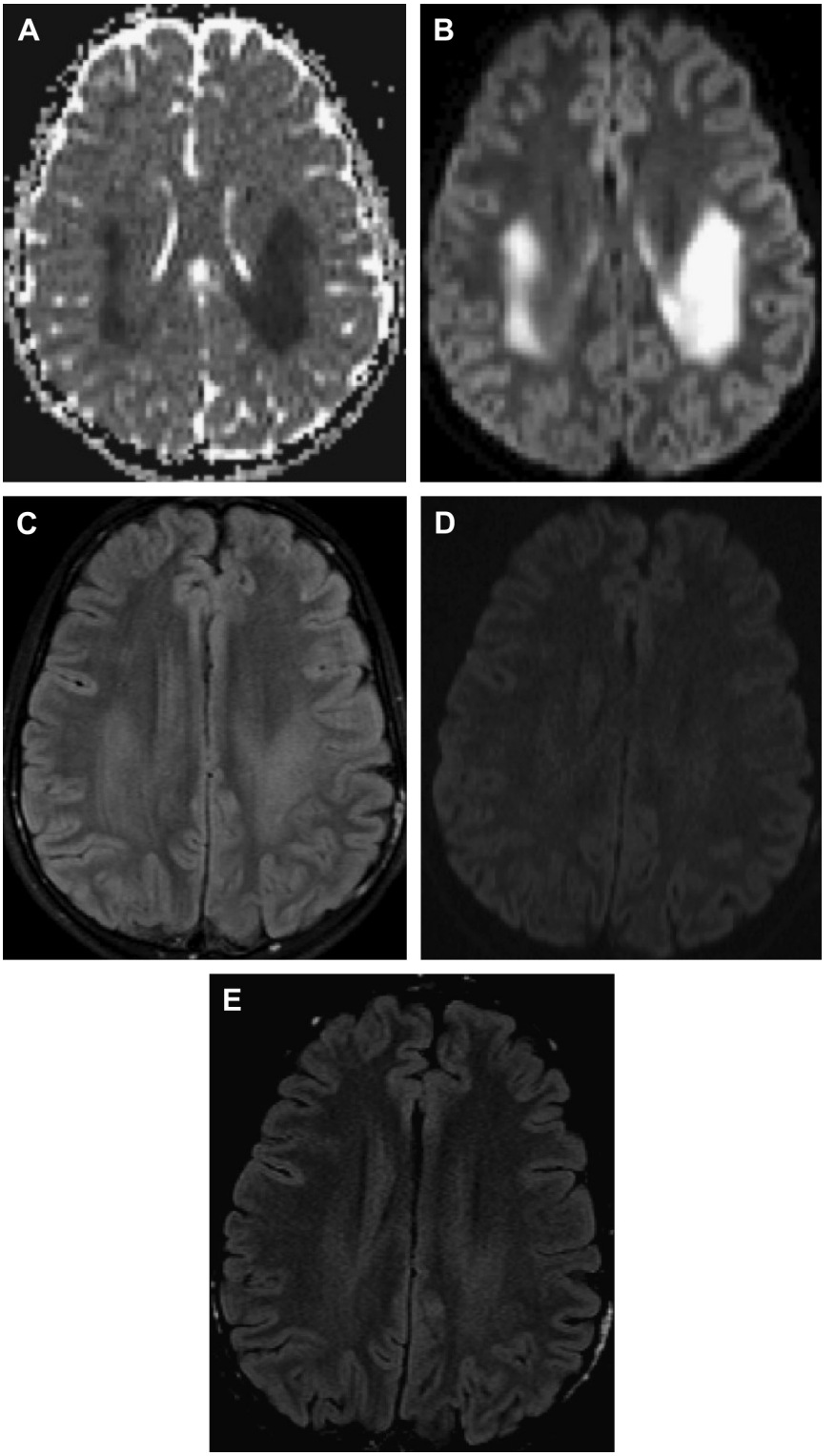

Fig. 3. Fourteen-year-old boy with acute neurologic deficit, eventually diagnosed with X-linked Charcot-Marie-Tooth. Apparent diffusion coefficient and trace diffusion imaging maps (*A, B*) demonstrate profound restricted diffusion in the centrum semiovale with only a faint FLAIR signal abnormality (*C*). Neurologic symptoms spontaneously resolved and the MR imaging 1 year later demonstrates normal diffusion-weighted image trace (*D*) and near normal FLAIR (*E*) appearance.

Box 6
Helpful clinical findings in leukodystrophies

Macrocephaly

Megalencephalic leukoencephalopathy with subcortical cysts
Canavan disease
Alexander disease
Mucopolysacchardoses (hydrocephalus)
GM2 gangliosidoses (Tay-Sachs, Sandhoff)
L-2-hydroxyglutaric aciduria
Glutaric aciduria type I

Microcephaly

Aicardi-Goutières syndrome
Menkes disease
Cockayne syndrome

Ophthalmologic Abnormalities

Cherry red macule: mucopolysaccharidosis, GM1/GM2 gangliosidoses, Niemann-Pick disease
Retinopathy/vision loss: mucolipidosis, dihydropyramidine dehydrogenase deficiency, trichothiodystrophy, Krabbe, vanishing white matter disease, giant axonal neuropathy, Pelizaeus-Merzbacher, Cockayne syndrome, peroxisomal biogenesis
Strabismus: succinic semialdehyde dehydrogenase
Nystagmus: Pelizaeus-Merzbacher, free sialic acid storage disorders, thiamine deficiency, infantile neuroaxonal dystrophy
Cataracts: Lowe syndrome, Cockayne syndrome, hypomyelination with congenital cataracts, trichothiodystrophy
Glaucoma: Lowe syndrome
Dislocated lens: hyperhomocysteinemia, molybdenum cofactor deficiency, isolated sulfite deficiency
Corneal opacification: mucolipidosis, mucopolysaccharidosis
Extraocular movement abnormalities; 18q deletion, mitochondrial disorder
Coloboma, megalocornea: dihydropyrimidine dehydrogenase deficiency

Dermatologic Abnormalities

Fucosidosis: trunk angiokeratoma
Methylmalonic acidemia: hair loss, desquamative dermatitis
Biotinidase: alopecia, rash
Menkes: sparse coarse hair with split ends, hypopigmented skin
Trichothiodystrophy: brittle hair, teeth/nail dysplasia, ichthyosis
Sjögren-Larsson: ichthyosis
Rhizomelic chondrodysplasia punctata: ichthyosis
Phenylketonuria: dermatitis, eczema
X-linked adrenoleukodystrophy: hyperpigmentation
Cockayne: photosensitivity
Aicardi-Goutières: chilblains (frostbite-like lesions)

Sensorineural hearing loss:

Trichothiodystrophy
Mitochondrial disorders
Peroxisomal biogenesis disorders

Data from Barkovich AJ, Patay Z. Metabolic, toxic, and inflammatory brain disorders. In: Barkovich AJ, editor. Pediatric neuroimaging. Philadelphia: Lippincott Williams & Wilkins; 2012. p. 81–239.

MBP resides in this region suggests a mechanism for the developmental disabilities experienced by these patients. There is an appearance of delayed myelination that is only visible to the naked eye on the T2-weighted images in the deep/subcortical white matter. The myelination pattern resembles an infant aged 1 to 1.5 years and does not progress beyond this point (**Fig. 5**).[34,35] Although the appearance suggests that haploinsufficiency of MBP is the sole explanation for delayed

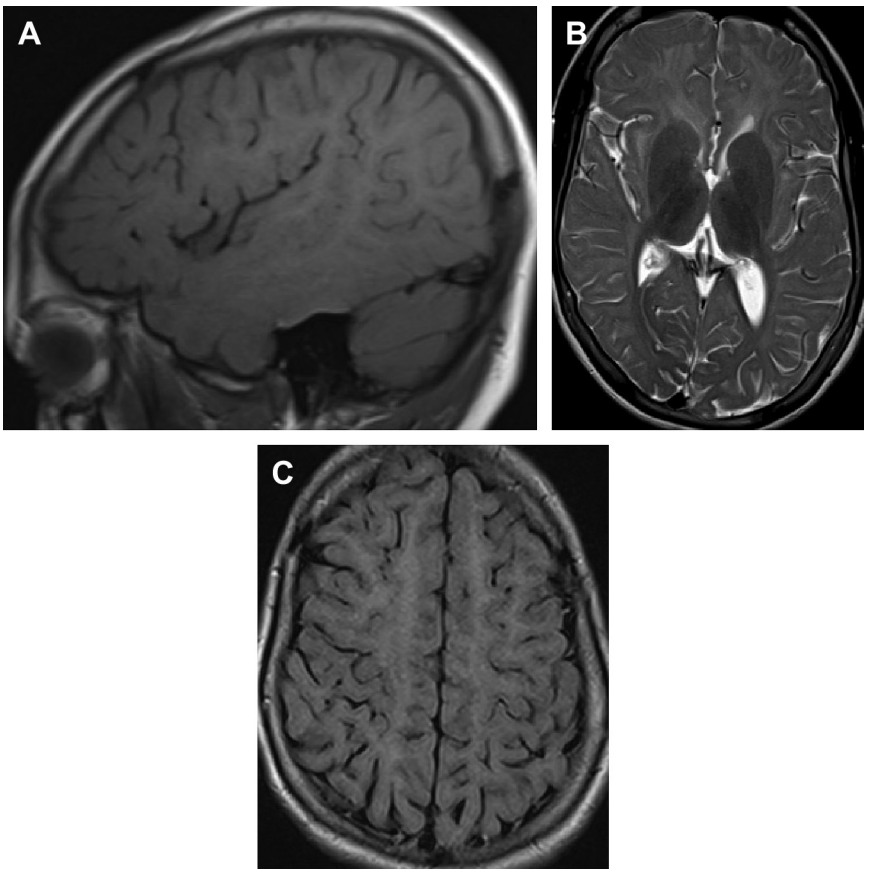

Fig. 4. Fourteen-year-old boy with classic Pelizaeus-Merzbacher disease, diagnosed after nystagmus noticed at 4 months of age. Although there is some myelination visible on sagittal T1-weighted imaging (*A*), the myelination resembles that of an infant on axial T2-weighted imaging (*B*). The degree of abnormality is particularly conspicuous on the fluid attenuated inversion recovery image (*C*), which demonstrates diffuse white matter hyperintensity resembling a T1-weighted image.

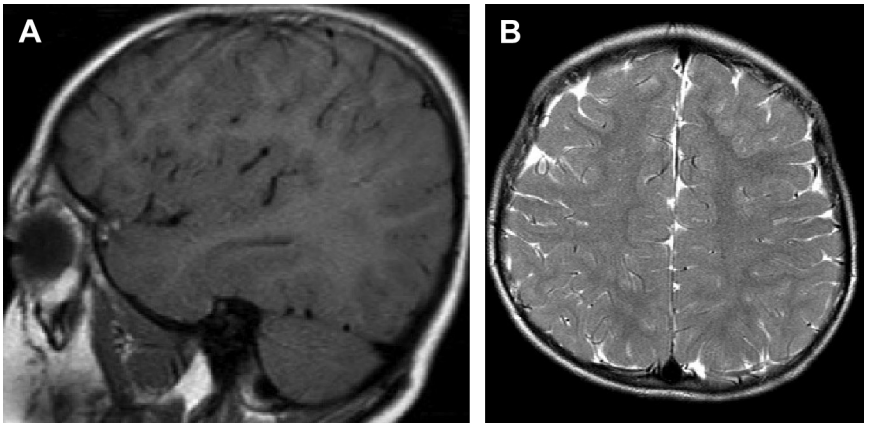

Fig. 5. Six-year-old boy with 18q22 deletion cleft lip, hypotonia, and developmental delay. Notice the normal myelination pattern on the sagittal T1-weighted image (*A*) but poor deep/subcortical white matter myelination on axial T2-weighted imaging (*B*).

myelination on T2-weighted images, an autopsy of a patient with 18q deletion syndrome found that the myelin sheaths were grossly intact on electron microscopy and myelin-sensitive stains.[36]

Free Sialic Acid Storage Disorders

Free sialic acid storage disorders are autosomal recessive disorders in which the transporter responsible for egress of sialic acid from lysosomes, sialin encoded by *SLC17A5* (6q13), is defective.[37] As a result, sialic acid builds up in lysosomes and spills into the circulation, where it is eventually excreted into urine. Three forms are recognized, in increasing severity: Salla disease largely as a result of a single point mutation endemic to Finland; an intermediate severity Salla disease; and infantile free sialic storage disease.[38] To avoid confusion with another disorder that lacks severe central nervous system (CNS) involvement and is caused by a separate enzyme, the term sialuria is avoided here.[39] The mild Salla form of the disease presents in early infancy with developmental delays, hypotonia evolving to spasticity, ataxia, and nystagmus; near normal life spans have been reported. The infantile form is more severe with cardiomegaly, hepatomegaly, and even prenatal symptoms of hydrops. MR imaging of the brain in patients with free sialic acid storage resembles PMD in that brain myelination appears arrested with a pattern resembling a child who is a few months old with thinning of the corpus callosum (**Fig. 6**); more severely affected patients appear even more immature and have some cerebellar volume loss.[40,41] The histologic basis of this MR imaging appearance is unclear. MR spectroscopy has demonstrated increased *N*-acetylaspartate (NAA) levels in patients with Salla disease attributed to overlap from sialic acid metabolites, an MR spectroscopy appearance consistently described for only 1 other disorder (Canavan disease).[42] Although often labeled sialuria, recent reports suggest that mild forms of Salla disease with arrested myelination can have normal urine sialic levels, something that should be considered during the workup of a patient with global myelination delay.[43]

Fucosidosis

Fucosidosis is an autosomal recessive lysosomal disorder caused by mutations in the α-L-fucosidase-1 gene *FUCA1* (1p34). Patients present either in the first year of life or shortly thereafter with intellectual and motor regression, eventually leading to spastic quadraparesis. Coarse facial features similar to mucopolysaccharidoses are also noted.[44] The imaging appearance is predominantly a nonspecific pattern of delayed myelination, but more pronounced periventricular signal increase has also been reported. Another characteristic finding is that of T2 hypointensity in the globus pallidus with variable increase in signal between the medial/lateral lamina of the globus pallidus and the medullary lamina of the thalamus (**Fig. 7**).[44–46] Although the hypointensity of the deep gray matter bears some superficial resemblance to the gangliosidoses and Krabbe disease discussed later, these 2 disorders lack the generalized myelination delay pattern, and

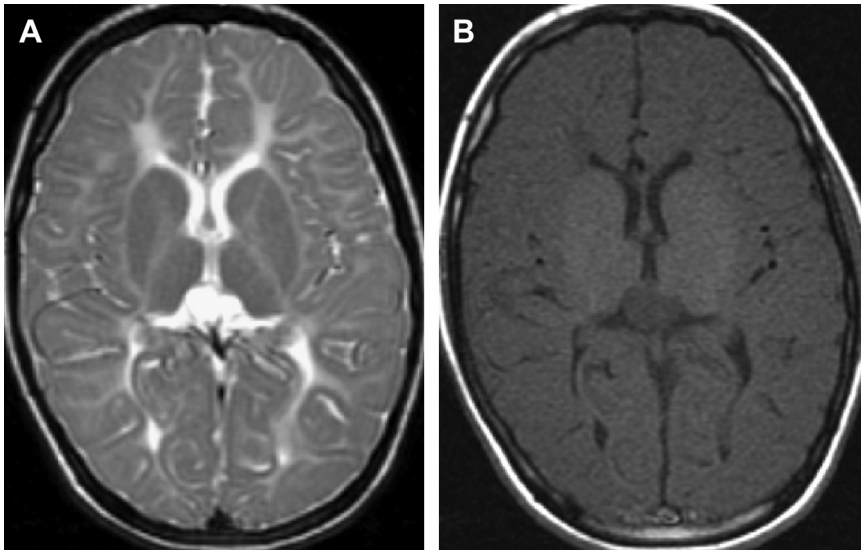

Fig. 6. Seven-year-old girl with developmental delay and Salla disease diagnosed at 3 years of age. Axial T2-weighted (*A*) and T1-weighted (*B*) images demonstrate absence of normal myelination.

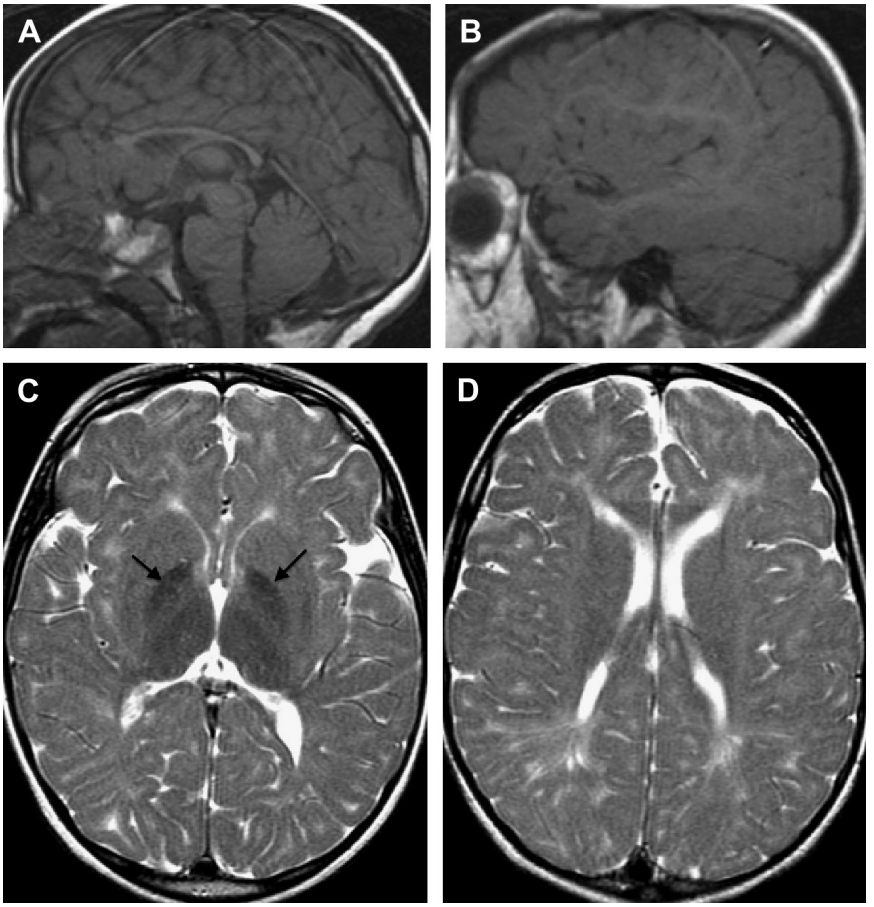

Fig. 7. Five-year-old boy with developmental delay/regression, subsequently diagnosed with fucosidosis. Sagittal T1-weighted images (*A, B*) demonstrate a thin corpus callosum and grossly normal myelination on T1-weighted imaging. Axial T2-weighted images (*C, D*) demonstrate hypointensity of the globus pallidus (*arrows*) for age with global decrease in myelination. Some of the periventricular white matter has increased T2 signal greater than hypomyelination, suggestive of gliosis. Cerebellar volume is intact.

they also have more pronounced basal ganglia hyperintensity. MR spectroscopy is also unique in fucosidase reflecting buildup of fucose with a doublet at 1.2 ppm and 3.4 to 3.8 ppm.[47,48]

Other Disorders with Delayed/Arrested Myelination

Additional monogenic disorders with delayed myelination have been reported. One of these disorders has been dubbed Pelizaeus-Merzbacher like disease (PMLD) and is caused by autosomal recessive mutations in *GJA12/GJC2* (1q42), a gap junction protein.[49,50] Other hypomyelinating disorders that have also be suggested as being Pelizaeus-Merzbacher like include a deletion syndrome involving heat shock protein *HSPD1*,[51] an X-linked deficiency in CNS thyroid transport due to *MCT8*,[52] and a hypomyelinating disorder caused by mutations in the tRNA synthesis and signaling protein *AIMP1/p43*.[53] The latter 2 disorders could be questioned as PMLDs because they feature some catchup myelination and microcephaly, respectively. Other hypomyelinating disorders are associated with distinctive clinical features: hypodontia and hypogonadism with the so-called 4H syndrome due to RNA polymerase III subunits *POLR3A/B*[54,55]; brittle hair and ichthyosis in the trichothiodystrophies seen with defects in 1 of at least 4 DNA repair enzymes[56]; hypomyelination with congenital cataracts (HCC) caused by mutations in *FAM126A* (7p21)[57]; and deep gray matter and cerebellar atrophy in hypomyelination with atrophy of the basal ganglia and cerebellum (H-ABC) recently mapped to mutations in *TUBB4A* (19p13).[58,59] Another disorder that can present as arrested myelination is nonketotic hyperglycinemia (deficiency of components of

the glycine cleavage system at 3p21, 9p24, 16q23).[60] This disorder exhibits restricted diffusion at sites of myelination at the time of imaging (eg, posterior limb of internal capsule and central tegmental tracts at the classic neonatal presentation)[61,62] and exhibits a characteristic glycine peak on MR spectroscopy at 3.56 ppm, suggesting the diagnosis.[10,63,64] An analysis of several hypomyelinating disorders has identified some unique features that may suggest a specific hypomyelinating disorder.[45] For example, 4H syndrome is distinguished from PMD, PMLD, and HCC by myelination of the optic radiations and posterior limb of the internal capsule with cerebellar atrophy and prominent T2 hypointensity of the ventrolateral thalamus (**Fig. 8**). As explained later under pattern 3 Cockayne syndrome clearly presents as generalized arrest in myelination for many patients, but other patterns can be observed.

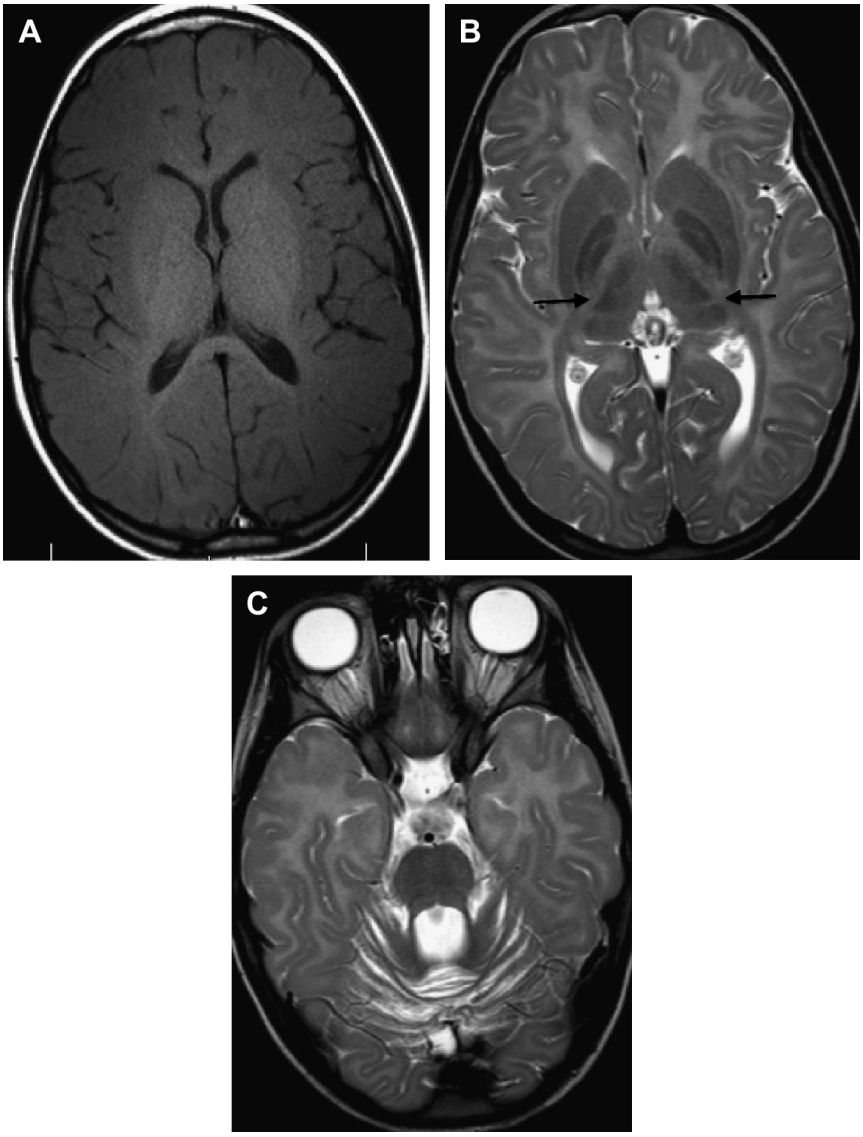

Fig. 8. Five-year-old girl with failure of incisor eruption, motor delay, and (subsequently) delayed puberty. Later diagnosed with 4H syndrome. Although there is global delay of myelination, there is myelination of the posterior limb of the internal capsule on axial T1-weighted images (*A*) and the optic radiations in both axial T1-weighted and T2-weighted images (*A, B*). There is characteristic hypointensity of the ventrolateral thalamus on axial T2-weighted images (*B, arrows*) and volume loss of the cerebellum (*C*). Hypointensity of the globus pallidus is an inconsistent feature for this disorder.

PATTERN 2: SUBCORTICAL WHITE MATTER PREDOMINANT SIGNAL ABNORMALITY

Although T2 hyperintensity in both the subcortical white matter and gray matter structures is a feature of several disorders (see later discussion), abnormalities concentrated in the subcortical white matter only are relatively uncommon.

Galactosemia

Galactosemia is caused by autosomal recessive mutation in 1 of 3 genes: galactokinase or *GALK* (17q24), galactose galactose-1-phosphate uridyltransfersase or *GALT* (9p13), or UDP-galactose-4-epimerase known as *GALE* (1p36). The most common form is the classic or type 1 galactosemia caused by *GALT* deficiency, which leads to buildup of galactose-1-phosphate and upstream metabolites such as galactitol.[65] The disease manifests on milk feedings with failure to thrive, poor feeding, lethargy, liver dysfunction, and eventually signs of cerebral edema. Even with institution of a lactose-depleted diet, neurologic sequela are common and include diminished intellectual achievement and decline, delayed speech, and cerebellar signs (ataxia, coordination problems).[66] The MR imaging findings resemble that of delayed terminal myelination with poor myelination in the subcortical white matter on T2-weighted imaging but grossly normal myelination on T1-weighted imaging (**Fig. 9**), corresponding to myelin pallor on pathologic examination.[67]

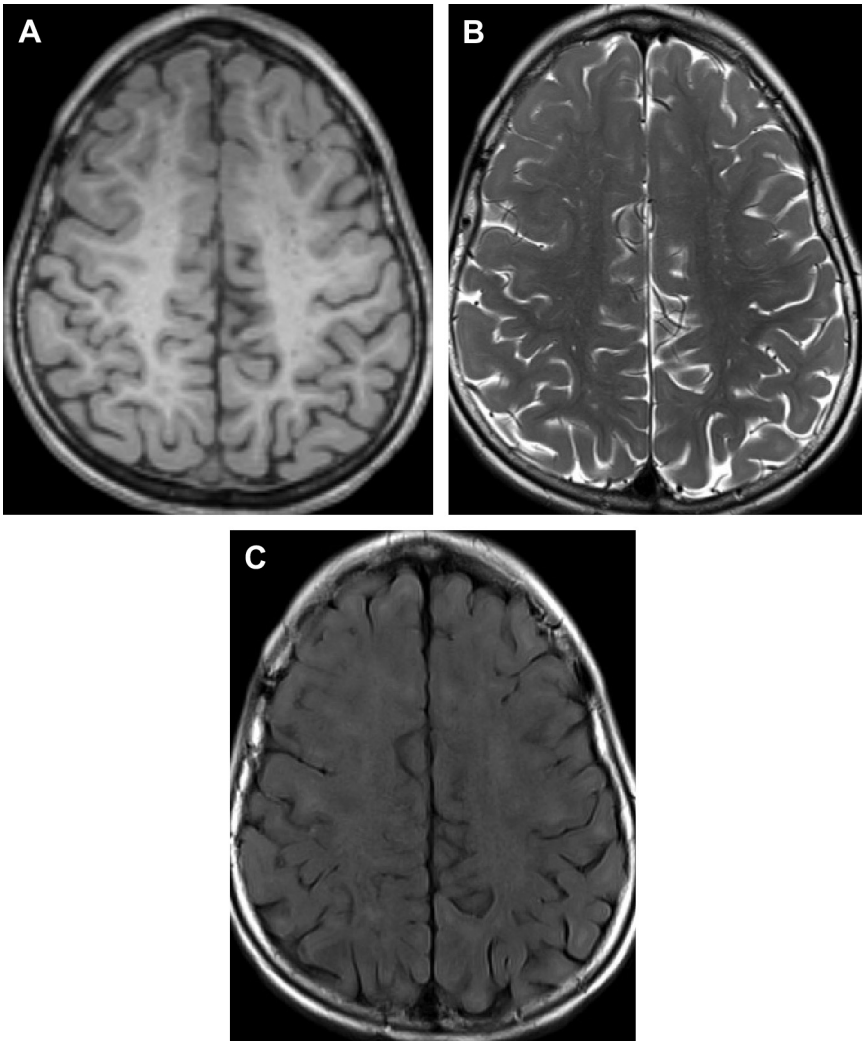

Fig. 9. Eight-year-old girl with galactosemia. Although the axial T1-weighted images suggest normal myelination (*A*), there is poor gray-white matter differentiation on the axial T2-weighted images (*B*) suggesting diffuse poor myelination of the subcortical white matter. These signal abnormalities are more conspicuous on the axial fluid attenuated inversion recovery images (*C*) where there is patchy signal increase.

However, the subcortical white matter often appears slightly heterogeneous on fluid attenuated inversion recovery (FLAIR) images, which is not expected for delayed myelination alone. Hyperintensity on T2-weighted imaging is lower in signal intensity than seen in other leukodystrophies with subcortical white matter predominance. MR spectroscopy can be helpful in securing a diagnosis as untreated patients are reported to have prominent galactitol peaks, a finding that resolves with initiation of a galactose-free diet.[68,69]

Megalencephalic Leukoencephalopathy with Subcortical Cysts

Megalencephalic leukoencephalopathy with subcortical cyst (MLC) is a rare disorder originally characterized as an autosomal recessive disorder secondary to mutations in *MLC1* (22q13), a transmembrane protein involved in regulation of cellular water balance.[70,71] The resulting disorder is interesting for minimal initial symptoms other than large head size when patients present during infancy. However, patients eventually manifest slight delay in achieving motor milestones as well as mild cognitive delay. After a period of several years, there is usually deterioration in motor (ataxia, spasticity) and cognitive function as well as a high incidence of seizures. Imaging findings include expansile T2 signal abnormality in the subcortical and deep white matter, sparing the most central/periventricular white matter and the occipital white matter. There is associated cystic change in the subcortical white matter in the temporal lobes and to a lesser extent, the frontoparietal lobes (**Fig. 10**).[72] Over time, atrophy ensues. Although this scenario accounts for approximately 75% of patients with MLC, a small group of patients with similar imaging findings lack *MLC1* mutations and have milder clinical and imaging phenotypes (eg, fewer or no cysts, abating white matter changes). Recently,

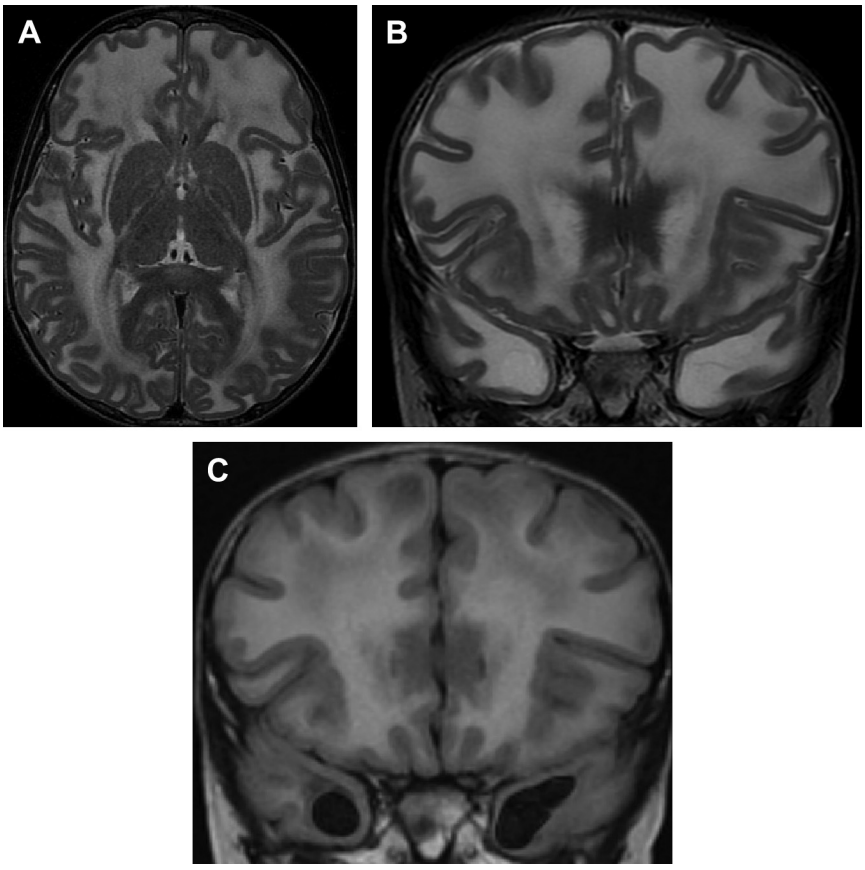

Fig. 10. Megalencephalic leukoencephalopathy with cysts in a 3-year-old child with >97th percentile head circumference and frequent falls/imbalance. Notice the expansile white matter signal abnormality greatest in the frontal lobes on the axial and coronal T2-weighted images (*A, B*). In the temporal lobes there is cystic degeneration best seen on the coronal FLAIR image (*C*).

autosomal dominant mutations in a trafficking protein for MLC1 known as *HEPACAM* were identified as 1 cause for this milder phenotype.[73]

Aicardi-Goutières Syndrome

Aicardi-Goutières syndrome (AGS) was originally described as a pseudo-TORCH syndrome affecting multiple members of a single family without evidence of an inciting infection and has since been recognized in other individuals.[74,75] The patients most often present in early infancy with irritability, sterile pyrexia, truncal hypotonia, extremity spasticity, and cognitive disability proportionate to the progressive microcephaly that is often present.[76] To date, mutations in 6 different genes have been identified that account for approximately 90% of cases of AGS: *TREX1* (3p21),[77] *RNASEH2A-C* (19p13, 13q14, and 11q13),[78] *SAMHD1* (20q11),[79] and *ADAR1* (1q21).[80] Although there can be some variability in severity of disease for any given AGS mutation,[81] *TREX1* mutations generally have more severe (neonatal) disease, whereas *RNASEH2B* typically have milder phenotypes.[82] Mutations in these genes trigger an activated immune response with increased CSF interferon-α and neopterin levels as well as histopathology suggesting small vessel vasculopathy and leptomeningitis, findings presumed related to the role the AGS gene products play in metabolizing DNA and RNA strands that can trigger an antiviral response.[76,83–85] Imaging evaluation of patients with AGS is notable for subcortical white matter signal abnormality, frontal/temporal pole predominance, and cystic change in patients with early (<3 months) onset of symptoms (**Fig. 11**).[86] All patients with AGS have parenchymal calcifications, primarily in the putamen but also within the dentate nucleus and deep white matter. Although atrophy is almost

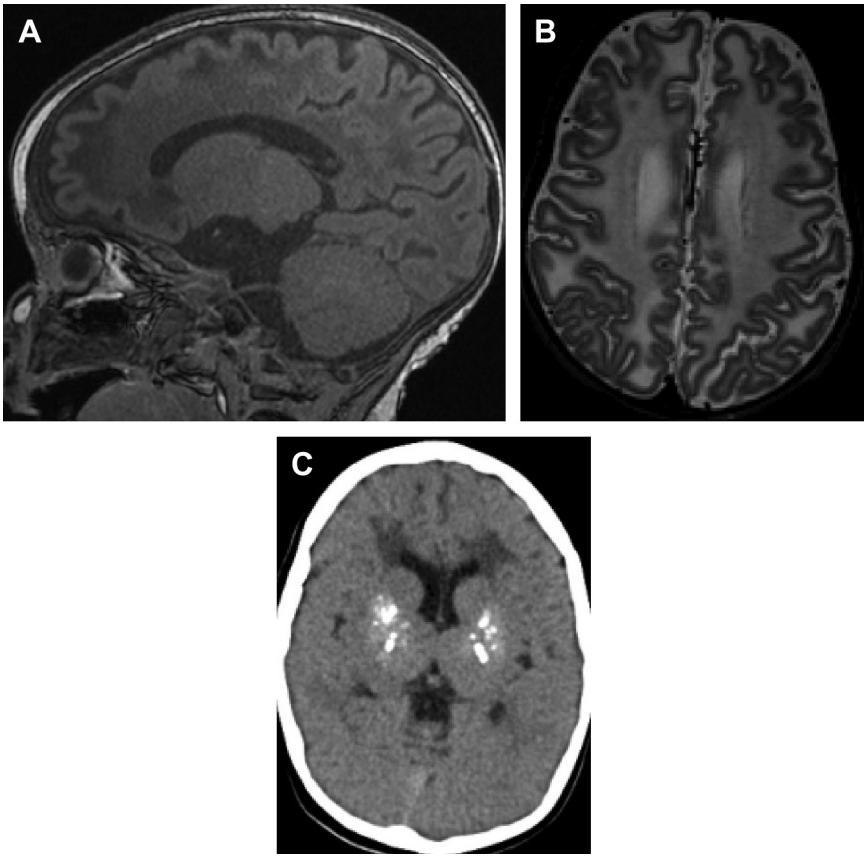

Fig. 11. Presumed case of Aicardi-Goutières syndrome in a patient with microcephaly, hypotonia, developmental delay, and increased CSF neopterin levels. Sagittal T1 (*A*) and axial T2 (*B*) MR imaging images at 5 months demonstrate white matter signal abnormality concentrated in the subcortical region, particularly in the frontal lobes. Computed tomography images from the same patient at 2 years of age (*C*) demonstrate basal ganglia calcifications.

universally present, it was progressive in only a third of the cases from the largest case series so far, possibly reflecting extent of disease at the time of imaging.

PATTERN 3: CENTRAL WHITE MATTER PREDOMINANT SIGNAL ABNORMALITY, WITH OR WITHOUT BRAINSTEM INVOLVEMENT

X-linked Adrenoleukodystrophy

Adrenoleukodystrophy (ALD) is an X-linked recessive disorder caused by mutations of the *ABCD1* gene (Xq28), a peroxisomal membrane transporter required for catabolism of very long chain fatty acids (VLCFA). As a result, there is buildup of VLCFAs detectable in the serum and a related inflammatory demyelination of the brain and atrophy of the adrenal glands.[87,88] In children, the disorder typically manifests in 5- to 10-year-old boys as a mild cognitive (learning) disorder or hyperactivity followed by progressive dementia and loss of motor function leading to quadraparesis. Most children will also have accompanying adrenal insufficiency at some point in their illness including the skin bronzing typical of corticotrophin hypersecretion, and a subset of patients present with adrenal symptoms only.[89,90] These childhood cases have a unique 3-layered pattern of cerebral white matter involvement concentrated in the parietooccipital lobes, classically first involving the splenium: a T2 hyperintense peripheral region of T2 hyperintensity corresponding to zone A where active demyelination occurs; an enhancing and diffusion-restricting rim called zone B where active inflammation occurs; and a central zone C with T2 hyperintensity corresponding only to gliosis at pathology (**Fig. 12**).[91] Although highly characteristic of ALD, a similar imaging appearance can be rarely encountered with mutations in a peroxisomal fatty acid enzyme, acyl-coenzyme A oxidase 1 *ACOX1* (17q25),[92] Recent work has shown that mild mutations in peroxisomal genes other than *ABCD1* can also have similar appearances (T2 hyperintensity of posterior periventricular white matter, splenium, dentate, superior cerebellar peduncle) even in the presence of seemingly normal peroxisomal serum metabolites.[93] Although this pattern is fairly well known for childhood ALD, it is less widely known that half of ALD patients present in adulthood with milder symptoms that typically manifest as lower extremity paresis, bowel/bladder dysfunction, and (in most cases) Addisonian symptoms. Only about half of these adult patients have brain MR imaging abnormalities with greatest signal abnormality in long tracts (including corticospinal tract) of the brainstem (adrenomyeloneuropathy) and portions of the cerebellum.[94,95] Other less common patterns of ALD include a frontal-predominant variant.[96]

Mucopolysaccharidoses

The mucopolysaccharidoses (MPS) are a collection of disorders caused by failed intralysosomal breakdown of various glycosaminoglycan molecules attached to proteoglycans (glycosylated proteins). Currently classified into 6 major subgroups depending on the specific enzyme (I, II, III, IV, VI, and VII), they are all transmitted in a recessive fashion although type II Hunter disease is X-linked. MPS types I, II, III, and VII are notable for their predominance of CNS morbidity, whereas types IV and VI (Morquio and Maroteaux-Lamy, respectively) feature more predominant musculoskeletal abnormalities, including spine abnormalities such as congenital kyphosis or stenosis from dural thickening. Among the CNS-predominant MPS variants, there is a wide spectrum of disability varying from normal intelligence in MPS I-S Scheie disease to severe mental retardation in MPS IH Hurler and MPS IIA Hunter forms of the disease. Associated abnormalities of the different mucopolysaccharidoses include facial dysmorphism, extremity contractures, corneal clouding, airway obstruction, hepatosplenomegaly, dural thickening, and hydrocephalus; these symptoms are attributed to abnormal deposit of glycosaminoglycans in patient tissues.[97,98] On brain imaging, patients with MPS typically have generalized decrease in gray/white matter differentiation, attributed to dysmyelination and faint diffuse increase in the T2 signal of the cerebral white matter.[99–104] This finding, as well as that of more pronounced T2 hyperintensity in the periventricular white matter, is fairly nonspecific. However, cystic enlargement of the perivascular spaces (particularly posteriorly) can be extremely conspicuous in the cerebral white matter and corpus callosum (approximately two-thirds of patients according to available case series[101,102,104]), suggesting the diagnosis of MPS. This spectrum of white matter disease in MPS is illustrated in **Fig. 13**. Intuitively, worsening white matter signal abnormality, volume loss, and nonspecific MR spectroscopy findings are found to correlate with worse cognitive impairment in at least some patients with MPS.[103,105]

Lowe Syndrome (Oculocerebrorenal Syndrome)

Lowe syndrome is a rare disorder caused by X-linked recessive mutation in an inositol polyphosphate 5-phosphatase encoded by *ORCL1*

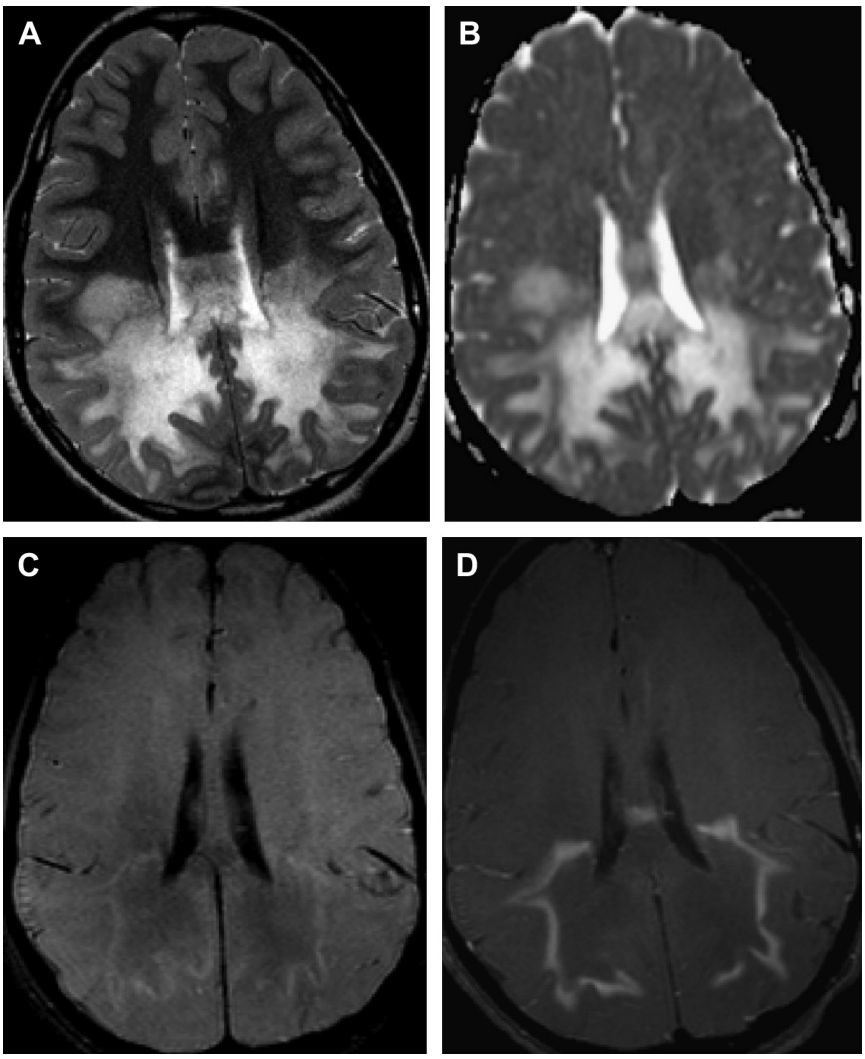

Fig. 12. Childhood X-linked adrenoleukodystrophy in a 10-year-old boy presenting with vomiting. The axial T2 image (*A*) demonstrates parietooccipital central white matter signal abnormality involving the posterior corpus callosum. Within this signal abnormality, there is a subtle hypointense band of white matter corresponding to faint restricted diffusion on the axial apparent diffusion coefficient diffusion maps (*B*) and enhancement after contrast injection (*C, D* precontrast and postcontrast axial T1 with fat saturation). This band of enhancement corresponds histologically to zone B, the inflammatory zone. The demyelinating zone A is peripheral and the gliotic zone C is deep to zone B.

(Xq28).[106,107] Affected patients have congenital cataracts and hypotonia with varying levels of mental retardation. There is eventual development of proteinuria (Fanconi syndrome) and frequently glaucoma also.[108] Although known cases number less than 200, the distinctive clinical findings and MR imaging findings make imaging diagnosis possible. Specifically, there is an unusual combination of periventricular signal increase with interspersed dilated perivascular spaces[109–111] although we have encountered molecularly confirmed instances of this disorder without the latter feature (**Fig. 14**). Elevated peaks at 3.56 ppm have been detected in these patients, possibly representing a phosphatidyl inositol 4,5-biphosphate resonance as opposed to the myoinositol peak normally located at this position.[112,113]

X-linked Charcot-Marie-Tooth

X-linked Charcot-Marie-Tooth (CMTX1) is an X-linked dominant form of Charcot-Marie-Tooth disease, a group of peripheral neuropathies. The

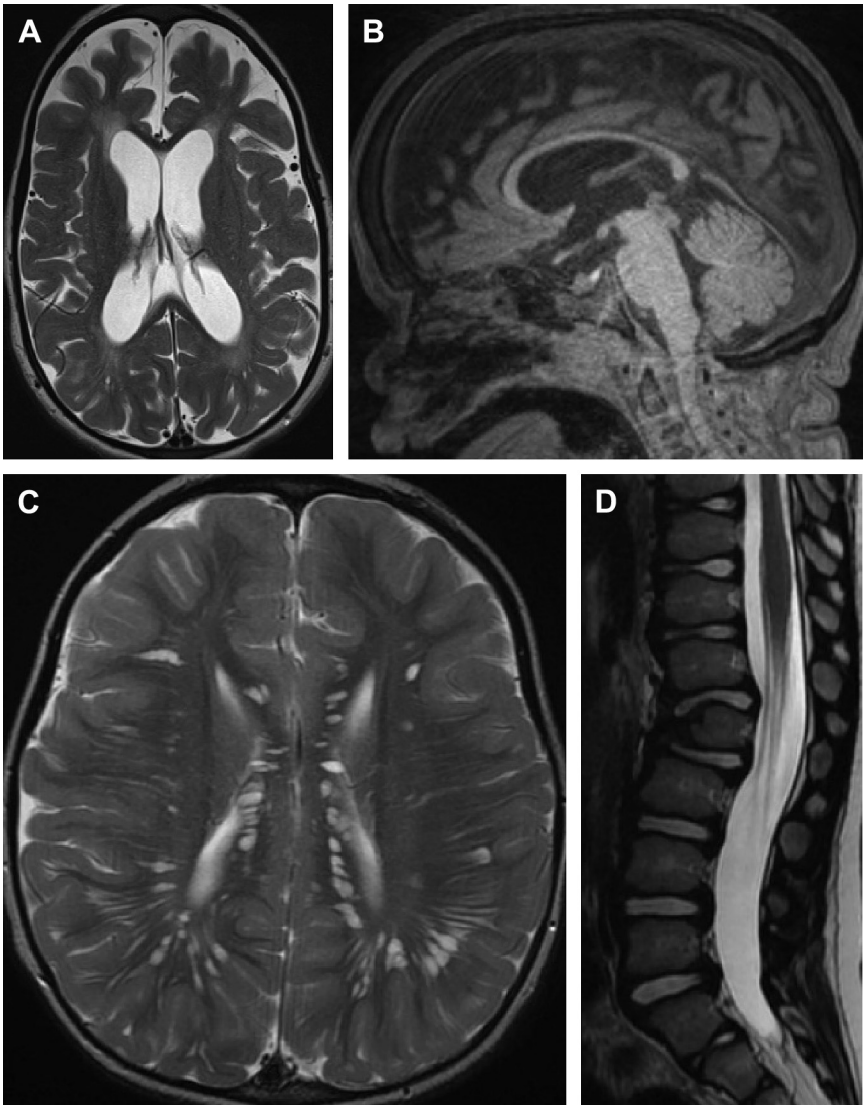

Fig. 13. Spectrum of white matter findings in mucopolysaccharidoses. MPS 1H Hurler in a 6-year-old girl with declining speech production and weakness: Mild ventriculomegaly, poor gray-white differentiation, and nonspecific periventricular white matter signal increase are noted on the axial T2-weighted image (*A*). Sagittal T1 image of the same patient (*B*) demonstrates frontal bossing, J-shaped sella, and crowding of the cervicocranial junction. MPS II Hunter in a 4-year-old boy. Axial T2-weighted image (*C*) demonstrates dilated perivascular spaces and sagittal T2 spine; (*D*) demonstrates a gibbus deformity.

disease is caused by mutations in the *CX32* gene, which encodes a neuronal gap junction protein.[114] Clinical symptoms typically manifest in the first few decades of life as a lower extremity predominant polyneuropathy with symptoms such as sensory loss, ankle drop, pes cavus, and muscle atrophy (eg, calf muscles and intrinsic hand muscles).[115] These symptoms are slowly progressive but do not seem to significantly diminish life expectancy.[116] Patients with CMTX come to radiologists' attention for occasional periods of focal neurologic deterioration after minor stressors (infection, trauma, high altitude) featuring weakness, ataxia, and even cranial nerve deficits. These symptoms often trigger a stroke evaluation. Symmetric deep white matter and callosal (splenial) T2 hyperintensity and restricted diffusion seen on MR imaging during episodes of acute deterioration suggests a toxic/metabolic cause rather than an infarction. There is spontaneous resolution of the

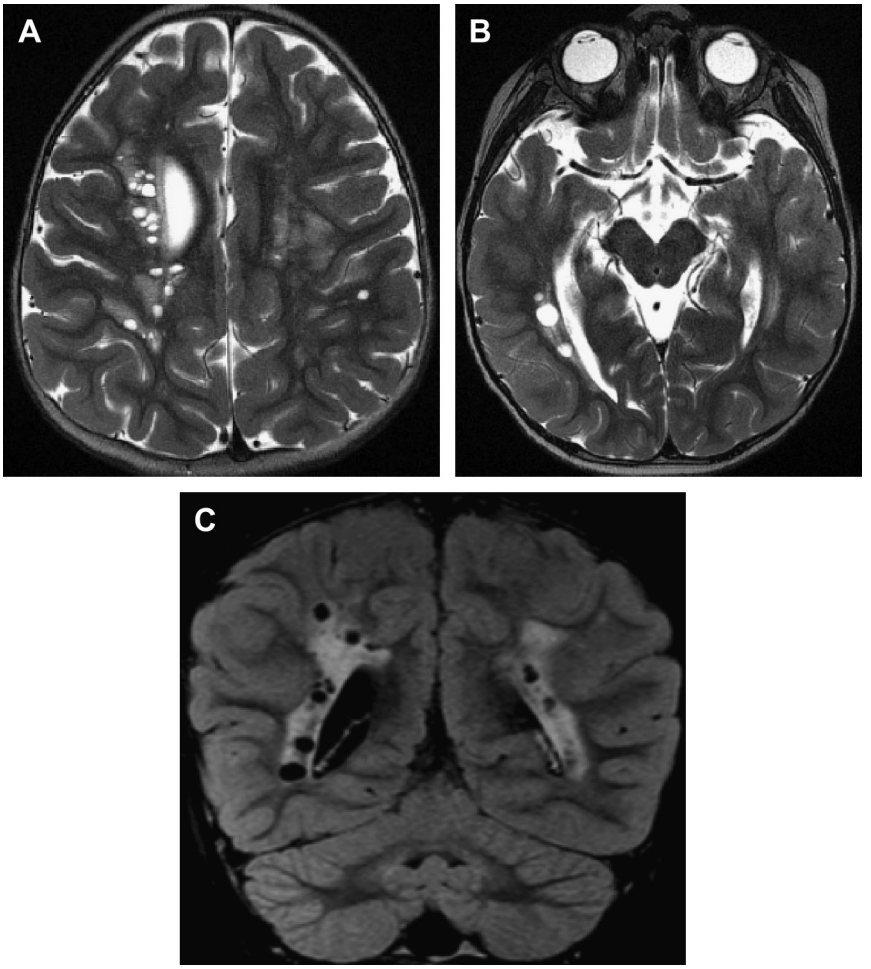

Fig. 14. Four-year-old with Lowe syndrome (seizure, Fanconi syndrome, cataracts). Axial T2 images (*A, B*) and coronal FLAIR (*C*) demonstrate periventricular signal abnormality with interspersed areas of cystic change. Note the lens prostheses in *B* from previous cataract surgery.

clinical symptoms and the MR imaging findings, the latter supporting myelin vacuolization rather than cytotoxic injury as the basis of the observed restricted diffusion (see **Fig. 3**).[117–119] Therefore, radiologists should be aware of this diagnosis because the imaging appearance is highly unusual in patients without toxin exposure, and clinical correlation (eg, symptoms in relatives, pes cavus deformity) can help establish the diagnosis of what is a fairly benign disorder.

Cockayne Syndrome

Cockayne syndrome (CS) is an autosomal recessive disorder resulting from mutations in 1 of 2 nucleotide excision repair genes, *ERCC8* (5q11, CS genetic complementation group A) and *ERCC6* (10q11, CS complementation group B); these 2 complementation groups account for 35% and 65% of CS cases, respectively. Mutations in either 1 of these genes can present with 1 of the 4 recognized clinical subtypes of CS (in decreasing order of severity): cerebro-oculofacial syndrome (COFS), type II CS, type I CS, and type III CS. For COFS, there is in utero growth restriction and arthrgryposis with early demise. For the mildest type III CS, the symptoms may not manifest until early childhood and survival to adulthood is reported.[120] Although patient who present later with CS achieve more milestones and may be initially minimally cognitively impaired, all CS subtypes proceed to deterioration/regression with associated sensorimotor disturbances (truncal hypotonia, extremity spasticity, sensorineural hearing loss). Failure to thrive (cachectic dwarfism) is also a universal symptom

in these patients. Surprisingly, cancer is not a dominant feature.[121]

Although classified as a disorder of global myelination delay by many investigators, more recent data suggest a wider variation in appearance. Specifically, recent papers suggest that milder forms of CS may have patchy deep and periventricular white matter with sparing of the subcortical white matter.[122] They also suggest that bouts of active demyelination may occur in the subcortical white matter as manifested by restricted diffusion and focal edema.[123] Regardless of the pattern of the white matter abnormality, the degree of parenchymal volume loss is generally more severe in patients with more severe clinical subtypes of CS (eg, affecting the posterior fossa and brainstem in infancy), and it also tends to progress with time as one would expect.[122,124] The calcifications have greatest propensity for the putamen followed by caudate, dentate, and cerebral white matter.[122] In addition to differences in distribution of the white matter signal abnormality, some investigators have noted that AGS-related calcifications have a less homogeneous appearance than seen in CS.[124] A typical case of CS is shown in **Fig. 15**.

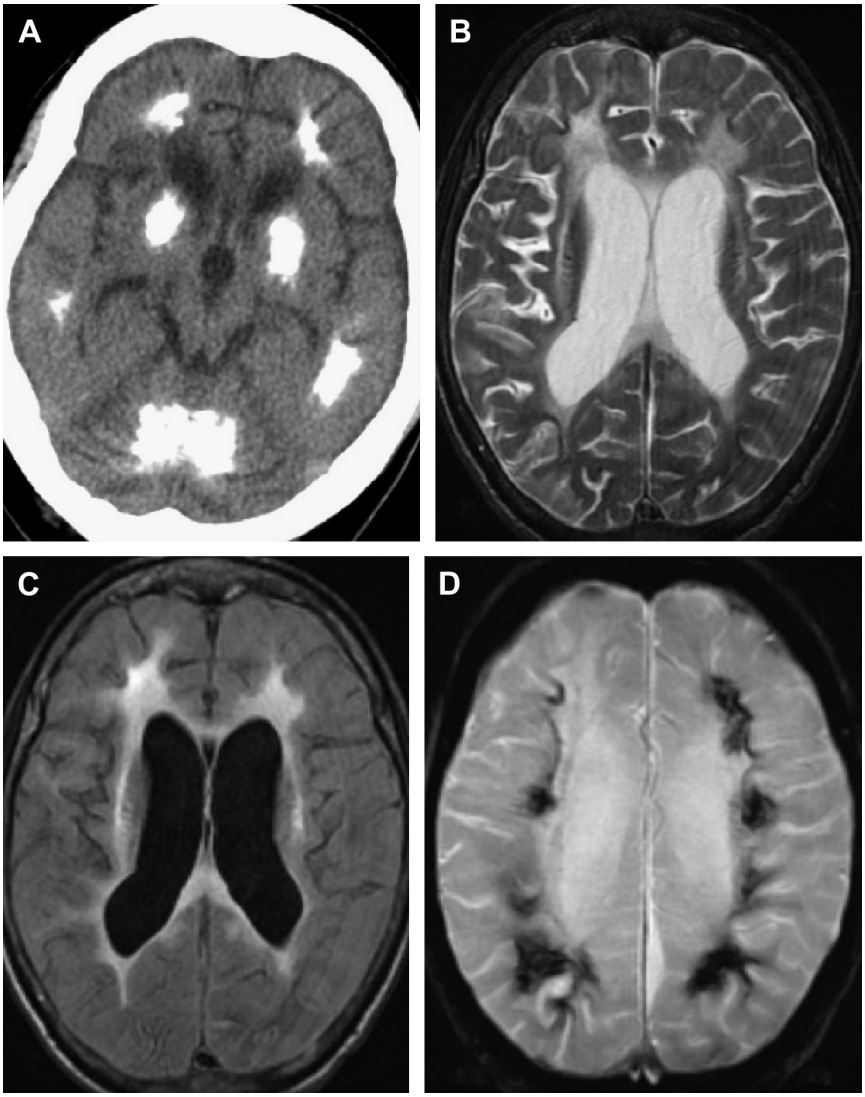

Fig. 15. Twenty-eight year old with Cockayne syndrome. Computed tomography of the head (*A*) demonstrates homogeneous coarse calcification of the basal ganglia, cerebral white matter, and cerebellar white matter. MR imaging of the brain demonstrates volume loss with central white matter signal increase on the axial T2 (*B*) and FLAIR (*C*) sequences. The T2* gradient recalled echo sequence (*D*) also demonstrates white matter calcification.

Leukoencephalopathy with Brainstem and Spinal Cord Involvement and Increased Lactate

Leukoencephalopathy with brainstem and spinal cord involvement and increased lactate (LBSL) is an autosomal recessive disorder caused by mutation in *DARS2*, a mitochondrial aspartyl-tRNA synthetase encoded on chromosome 1 (1q25).[125,126] Clinically, the disease manifests in late childhood with progressive ataxia and spasticity as well as impaired dorsal column function (eg, proprioception). Although exceedingly rare, this disorder does have a highly characteristic pattern of signal abnormality that allows it to be recognized on MR imaging and was used to define the disease entity (**Fig. 16**): patchy central white matter T2 hyperintensity sparing the subcortical U fibers with involvement of the dorsal/lateral columns of the spinal cord, medullary pyramids, and at least 1 minor location (splenium of the corpus callosum, medial lemniscus, spinocerebellar tracts in medulla, superior and inferior cerebellar peduncles, cerebellar white matter, parenchymal trigeminal nerve, and trigeminal tracts). Lactate on MR spectroscopy is almost always increased.[127] Restricted diffusion has been observed in some of the T2 hyperintense lesions.[128] The pattern of long tract involvement and deep gray structure sparing set this disease apart from leukoencephalopathies such as maple syrup urine disease (MSUD) and Krabbe disease (see later discussion) as well as inflammatory disorders such as acute disseminated encephalomyelitis. However, more severe infantile cases with genetic confirmation have been reported to involve the white matter more extensively and even extend into the globus pallidus, making imaging recognition of the disorder more challenging in this age group.[129] Also, LBSL has similarities to a recently described disorder, hypomyelination with brainstem and spinal cord involvement (HBSL), caused by the cytosolic aspartyl-tRNA synthetase *DARS*.[130] White matter involvement in HBSL appears more homogeneous than LBSL and can extend to the subcortical white matter.

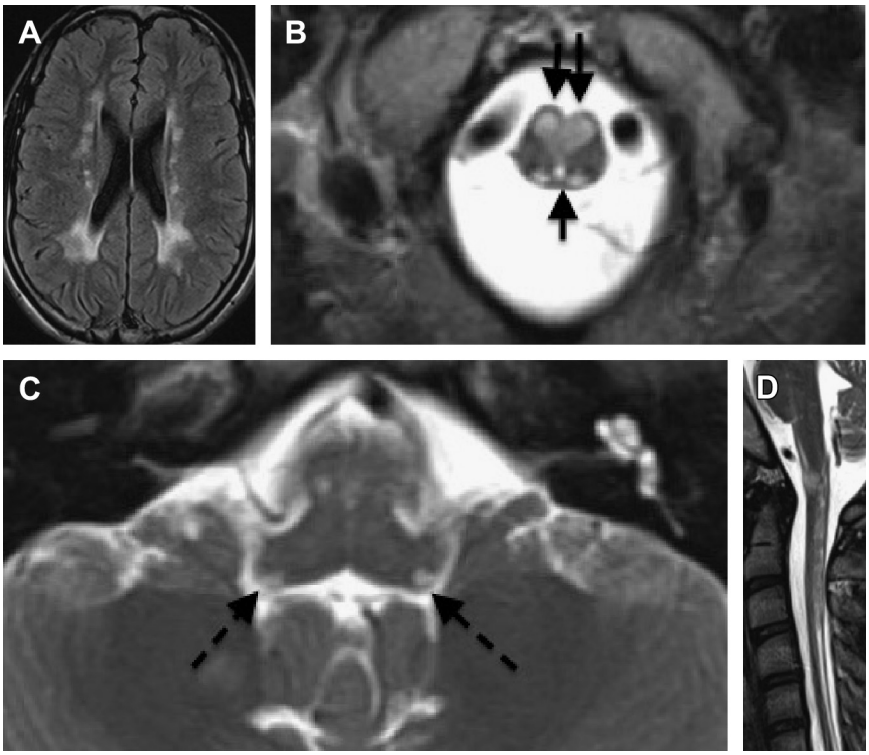

Fig. 16. Seventeen-year-old girl with leukoencephalopathy with brainstem and spinal cord involvement and increased lactate. Axial FLAIR image (*A*) demonstrates patchy central white matter signal increase. Axial T2-weighted images (*B, C*) demonstrate abnormal signal in the dorsal columns (*single arrow*), medullary pyramids (*double arrow*), and inferior cerebellar peduncle (*dashed arrows*). Dorsal column involvement is also visible on the sagittal T2 image of the cervical spine (*D*).

Other Leukodystrophies with Central White Matter Involvement

The pattern 3 diseases discussed thus far have unusual patterns of signal abnormality that make a specific diagnosis feasible. However, it is more common to encounter leukodystrophies with nonspecific periventricular and deep white matter signal increase. Some diseases in this category are illustrated in **Fig. 17**.

Metachromatic leukodystrophy (MLD) is perhaps the most common of these diseases, caused by mutations affecting *ARSA* or arylsulfatase A (22q13) with similar appearances seen in multiple sulfatase deficiency and saposin B deficiency.[131–134] Late infantile, juvenile, and adult onset forms of the disease are recognized; late infantile presentation is the most common (majority).[135,136] MLD forms all share progressive neurologic deterioration after an initial period of normalcy. In the late infantile form, this manifests as loss of milestones, hypotonia, and eventual cognitive impairment with spastic quadriparesis. The imaging manifestation is confluent signal abnormality in the deep and periventricular white matter with sparing of subcortical U fibers until the end stage of the disease.[137,138] The diagnosis may be suggested by cranial nerve or cauda equina enhancement, which is not commonly seen with other leukodystrophies.[10,139] Although

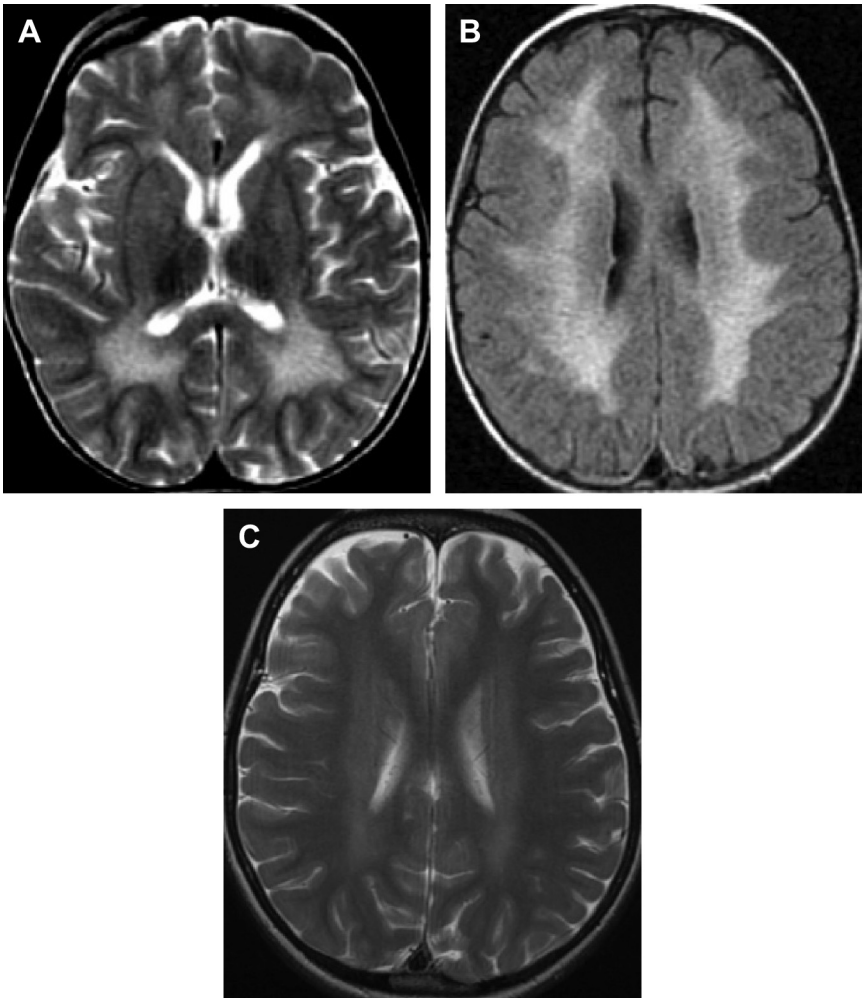

Fig. 17. Additional leukodystrophies with central white matter predominance. Three-year-old with metachromatic leukodystrophy, axial Fluid attenuated inversion recovery (FLAIR) (*A*) and T2 (*B*) images. Notice the sparing of the subcortical white matter and confluent appearance of the signal abnormality. Faint tigroid sparing can be seen along the perivascular spaces, particular on the FLAIR image. Neuronal ceroid lipofuscinosis typically presents as gray matter volume loss, but central white matter signal increase can occasionally be detected as in this axial T2 image of a 5-year-old girl with CLN8 (*C*).

some investigators believe that a tigroid sparing of the perivascular spaces of the affected white matter is characteristic for this disorder, there is pathologic and imaging evidence of such sparing in other leukodystrophies.[140–145]

Other disorders that primarily involve the central white matter include phenylketonuria (deficient phenylalanine hydroxylase, 12q23),[146,147] Sjögren-Larsson syndrome (deficient fatty aldehyde dehydrogenase, 17p11),[148] and hyperhomocysteinemia (multiple responsible enzymatic deficiencies).[149,150] MR spectroscopy can assist with detection of some of these disorders: Sjögren-Larsson has 0.9/1.3 ppm peaks that do not suppress at long TE.[151] Although the neuronal ceroid lipofuscinoses can be classified primarily as disorders of gray matter (cortical atrophy and deep gray hypointensity), deep/periventricular white matter signal abnormalities are seen in some of the 9 neuronal ceroid lipofuscinosis variants, mimicking other diseases discussed in this section.[152,153] Mild forms of vanishing white matter disease (autosomal recessive deficiency in 1 of 5 translation initiation factors, EIFB1-5)[154,155] can initially manifest as nonspecific central white matter signal increase.[156] The evolution to diffuse white matter involvement with cavitation eventually points to vanishing white matter disease, as does the characteristic history of stress-provoked worsening of ataxia/spasticity.

PATTERN 4: COMBINATIONS OF GRAY AND WHITE MATTER SIGNAL ABNORMALITY

Canavan Disease

Canavan disease is an autosomal recessive disorder caused by deficiency of aspartoacylase or *ASPA* (17pter-17p13), an enzyme responsible for degrading NAA.[157–159] The most common presentation is macrocephaly, hypotonia, and irritability before 6 months of age followed by spasticity, blindness, and (in some cases) seizures. The findings are attributed to buildup of NAA (both in the brain and peripherally in urine), a substance believed to cause spongiform changes of white matter as a result of osmotic shifts or impaired myelin synthesis.[160–162] Imaging findings of infantile Canavan disease are distinctive, featuring extensive subcortical white matter signal increase and appearance of mild gyral swelling as well as (almost invariably) globus pallidus T2 signal increase with sparing of the corpus striatum; over time, the white matter signal abnormality becomes more extensive and atrophy ensues (see **Fig. 2**). Occasionally, the brainstem and dentate nucleus may be involved.[163–165] Attenuated severity or atypical imaging patterns (eg, corpus striatum involvement) have been observed in mild cases of Canavan disease presenting later in childhood.[166–168] Typically, there is some restricted diffusion in the areas of signal abnormality resulting from intramyelinic edema believed to be caused by accumulation of NAA within neurons and increased water migration from the axon into the periaxonal space. Although these findings may resemble some other leukodystrophies (see L-2-hydroxyglutaric aciduria later), the macrocephaly and MR spectroscopy suggest the diagnosis. Specifically, there is a marked increase in NAA in Canavan disease,[169,170] a unique MR spectroscopy finding characteristic of Canavan and Salla diseases.

L-2-Hydroxyglutaric Aciduria

L-2-Hydroxyglutaric aciduria (L2HGA) results from autosomal recessive mutations in the mitochondrial enzyme L-2-hydroxyglutaric acid dehydrogenase (14q22); buildup of L-2-hydroxyglutaric acid results.[171] L2HGA typically presents in early childhood as motor delay and mild to severe mental retardation followed by progressive cerebellar dysfunction (ataxia) and movement disorder (tremor, choreoathetosis); seizure and macrocephaly are present in some patients.[172] MR imaging findings are distinctive if not pathognomonic. According to the largest review of L2HGA cases so far published, virtually all patients had T2 signal increase within the subcortical white matter (multifocal and frontal predominant initially), dentate nucleus, and basal ganglia (initially peripheral in the corpus striatum).[173] Although a similar appearance can be seen in Canavan disease and Kearns-Sayre (a mitochondrial disorder), the consistent presence of dentate signal abnormality and absence of brainstem involvement distinguishes L2HGA from these other possibilities (**Fig. 18**).[171,174] Isocitrate dehydrogenase (*IDH1/2*) mutations in low-grade gliomas, secondary glioblastomas, and leukemia are known to cause buildup of 2-hydroxyglutaric acid enantiomers. Although there does seem to be an association between L2HGA and primary brain tumors,[175] recent evidence suggests that the basis of IDH-related growth dysregulation is actually production of the *R*/D-2-hydroxyglutarate isomer.[176,177] Although similar sounding, D-2-hydroxyglutaric aciduria (deficiency of D-2 hydroxyglutaric acid dehydrogenase, 2q37) has a completely different and somewhat nonspecific imaging pattern: marked lateral ventriculomegaly and germinolytic cysts with delayed gyration and myelination.[178] Because of interest in using 2-hydroxyglutarate as a biomarker for IDH mutation–bearing gliomas, MR spectroscopy

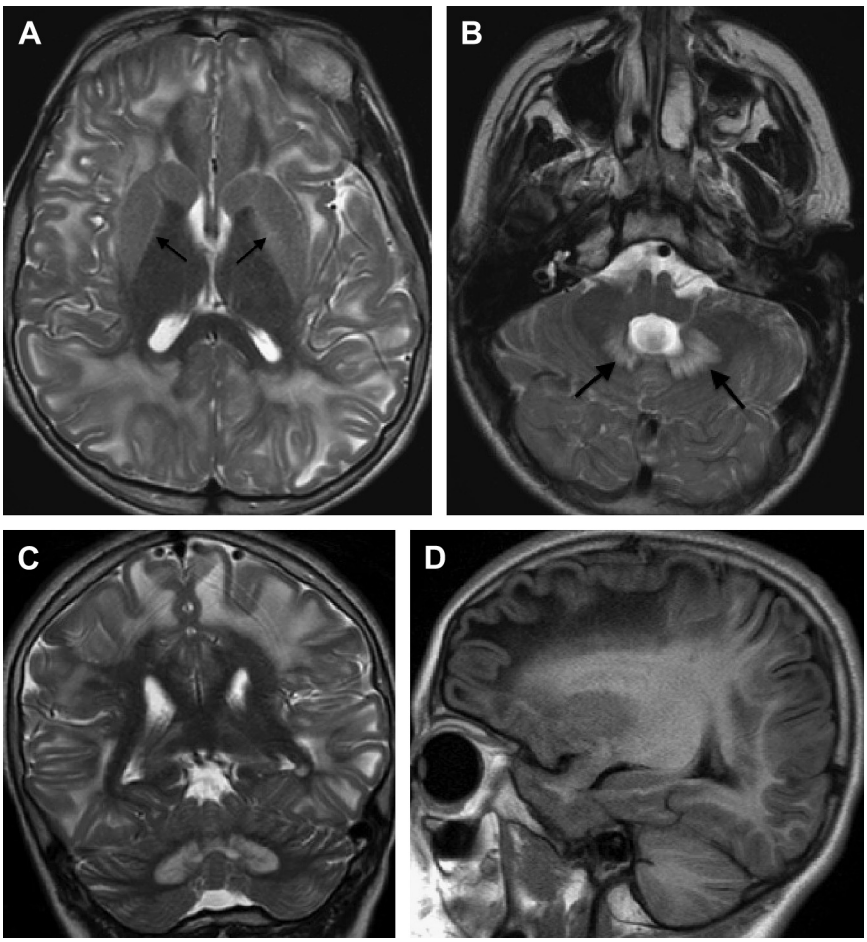

Fig. 18. L-2-hydroxyglutaric aciduria in a 13-year-old boy. Axial T2-weighted (*A, B*), coronal T2-weighted (*C*) and sagittal T1-weighted (*D*) images demonstrate subcortical white matter signal abnormality, frontal predominant and sparing the central white matter. There is also peripheral corpus striatum and dentate nucleus signal increase (*arrows*).

techniques have been developed for the detection of 2-hydroxyglutarate and may eventually become available for analysis of L2HGA also.[179,180]

Alexander Disease

Alexander disease is an autosomal dominant disorder caused by missense mutations in glial fibrillary acidic protein *GFAP* (17q21).[181–183] Mutations in this protein are believed to decrease GFAP solubility and trigger formation of inclusion bodies such as the Rosenthal fibers seen under the microscope in this disorder, leading to accumulation of abnormal astrocytes and myelin pallor throughout affected brain tissue.[184–186] Historically, 3 forms of Alexander disease are recognized: infantile with typical presentation before 6 months of age (51% of cases); juvenile (23% of cases); and adult (24% of cases).[187] As with the other leukodystrophies discussed, the earlier onset forms are associated with more severe symptoms. The typical infantile form presents with macrocephaly, failure to thrive, difficulty swallowing, loss of intellectual/motor milestones, lower extremity weakness, ataxia, seizures, and occasionally hydrocephalus. The juvenile and adult forms are dominated more by ataxia and bulbar/pseudobulbar symptoms as well as the seizures and lower extremity weakness seen in the infantile form; a small percentage of the juvenile but not adult patients also have macrocephaly.[182,187,188] Typical imaging characteristics include frontal-predominant subcortical to periventricular white matter T2 hyperintensity with swelling of the overlying gyri; swelling of the fornix and optic nerves; periventricular areas of T1/T2 shortening; deep gray matter signal increase or

atrophy; dentate hilum signal increase; brainstem (midbrain/medulla) signal increase; and enhancement of involved areas (**Fig. 19**). Progression to atrophy and occasionally white matter cavitation are common. These findings have been summarized in criteria designed to facilitate diagnosis using MR imaging in infantile and juvenile Alexander disease.[189] However, atypical presentations of Alexander disease (eg, posterior fossa and brainstem-predominant forms including some with tumefactive changes or a ventricular garland) have been recognized, particularly in juvenile forms of the disease.[18,190] Adult cases seem to be distinct in appearance, featuring primarily brainstem and cord atrophy with signal abnormality.[191,192]

GM1/GM2 Gangliosidoses (Tay-Sachs, Sandhoff Disease)

Gangliosides are minor myelin constituents that are composed of a glycosphingolipid (ceramide lipid bound to an oligosaccharide) and at least 1 sialic acid molecule. Autosomal recessive defects

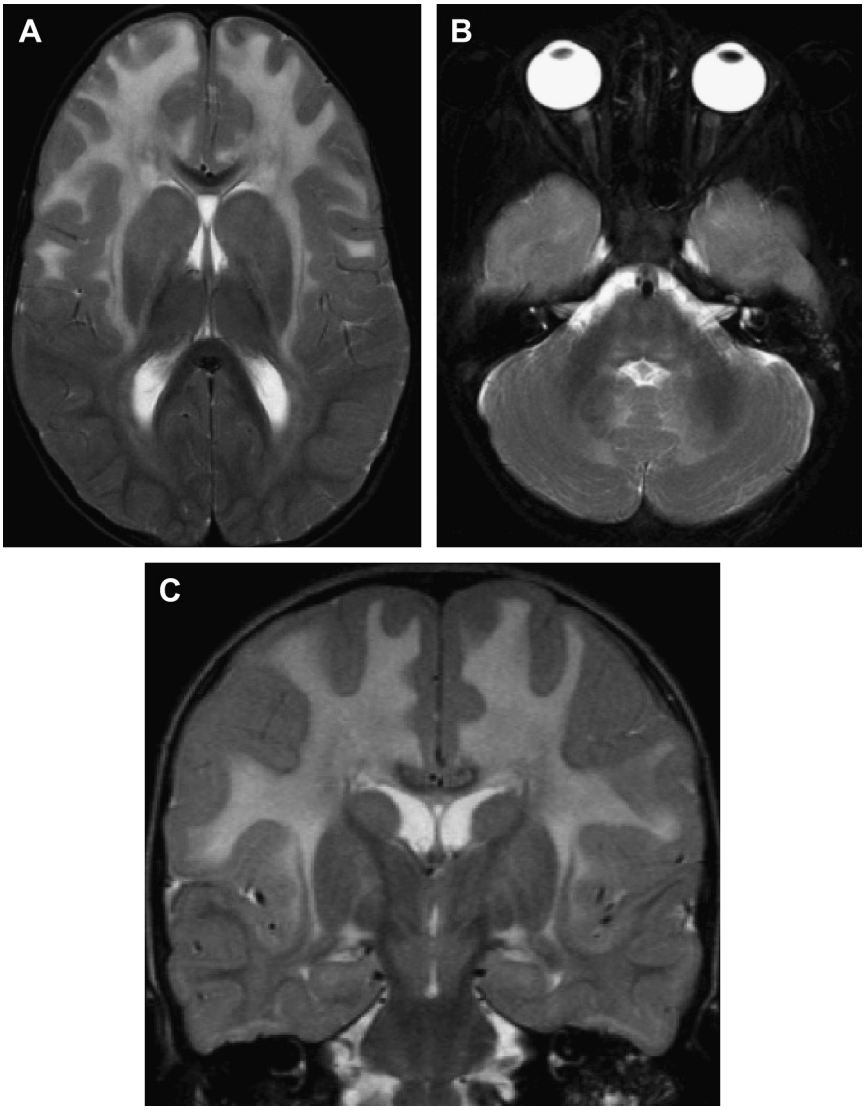

Fig. 19. Five-year-old child with Alexander disease. Axial (*A, B*) and coronal T2-weighted (*C*) images of the brain demonstrate expansile frontal subcortical white matter signal abnormality extending to the ventricle and signal increase within the basal ganglia, to a lesser extent also the brainstem. In the setting of macrocephaly, this appearance is virtually pathognomonic of Alexander disease. Other classic features not demonstrated in this case include enhancing areas of white matter T1/T2 shortening.

in the lysosomal enzymes that turn over the gangliosides lead to gangliosidoses.[188,193] GM1 gangliosidosis is caused by mutations in the lysosomal β-galactosidase *GLB1* (3p21),[194–196] the enzyme that degrades GM1 to GM2. GM2 gangliosidosis is caused by mutations in 1 of 3 gene products that control hexomindinase activity necessary to degrade GM2 to GM3: hexominidase A (15q23),[197–199] hexominidase B (5q13),[200,201] and the GM2 activator protein (5q31).[202–204] The GM2 gangliosidosis caused by hexominidase A deficiency is called Tay-Sachs disease, and the GM2 gangliosidosis caused by hexominidase B deficiency is called Sandhoff disease; hexominidase B forms heterodimers with the A isozyme as well as the B homodimers that have different substrates than the A/B heterodimer. The infantile forms of GM1 and GM2 gangliosidoses share similarities in that hypotonia and psychomotor retardation, early blindness, and peculiar startle responses are common. Eventually these infantile cases progress to spastic quadraparesis, seizures, and early death.[188,205,206] However, the GM1 gangliosidoses are somewhat distinct in that they have the hepatomegaly and kyphoscoliosis that resembles a mucopolysaccharidosis (*GLB1* mutations can cause a form of Morquio syndrome). GM2 gangliosidoses are distinctive for their higher incidence of cherry red maculae and macrocephaly although Sandhoff disease also features hepatosplenomegaly. The adult forms of the GM1/GM2 gangliosidoses are dominated by extrapyramidal symptoms (dystonia, choreoathetosis, ataxia); adult-onset GM2 gangliosidoses also have significant cognitive impairment and psychiatric disease.[204,207,208] The juvenile forms fall in between the infantile and adult forms of the disease.

Despite the differences in biochemistry and symptomatology, the neuroimaging features of the gangliosidoses are very similar. Infantile forms present with thalamic T1/T2 shortening attributed to mineralization and T2 hyperintensity of the basal ganglia. There is diffusely delayed white matter myelination, although myelination is preserved in the internal capsules, corpus callosum, and optic radiations (**Fig. 20**).[209,210] In some cases, the white matter T2 hyperintensity is greater than explained by a simple lack of myelination, a finding attributed to abnormal myelin turnover or demyelination.[188] This constellation of findings is characteristic for infantile GM1/GM2 gangliosidosis, but some unusual variant cases have been published (eg, lack of basal ganglia involvement[211]). Krabbe disease can resemble this disease, but the T2 hyperintensities of the basal ganglia and sparing of the corpus callosum are much less common.[188] Also, the thickening and enhancement of the cranial nerves and cauda equina seen in Krabbe disease is not present in the gangliosidoses. Adult forms of the gangliosidoses are notable primarily for faint diffuse cerebral white matter hyperintensity manifesting as poor gray-white matter

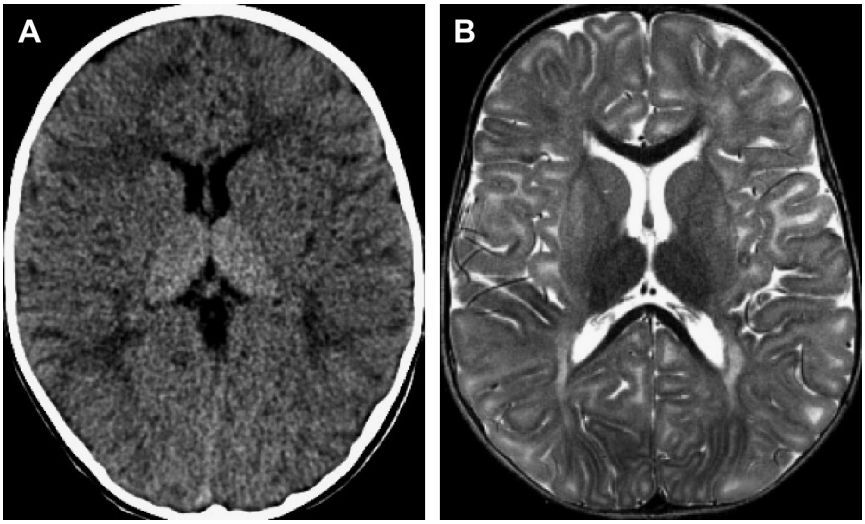

Fig. 20. GM2 gangliosidosis (Sandhoff disease) in a 14-month-old girl with seizures, cherry red macula, and hypotonia. Noncontrast computed tomography of the head (*A*) demonstrates hyperdensity of the thalami and a suggestion of white matter hypodensity. Axial T2 MR imaging of the brain (*B*) demonstrates T2 hypointensity of the thalami corresponding to the computed tomography finding as well as basal ganglia and subcortical white matter signal increase. Note that the internal capsules and corpus callosum remain normal in signal intensity.

differentiation and diffuse brain atrophy.[188] Differences between late-onset GM1 and GM2 include more conspicuous volume loss in the cerebellum for late-onset GM2 gangliosidosis,[207,212,213] and frequent reports of basal ganglia signal increase in late-onset GM1 gangliosidosis.[214,215] Juvenile and late infantile forms of GM1 can have similar appearance to either the infantile or adult onset forms of the disease.[210,216]

Krabbe Disease

Krabbe disease is a disorder caused almost exclusively by autosomal recessive deficiency of the lysosomal enzyme responsible for degrading the myelin constituent cerebroside into galactose and ceramide, β-galactocerebrosidase *GALC* (14q13).[217–219] The resulting enzyme deficiency leads to buildup of the toxic upstream metabolite psychosine and defective myelin turnover, associated with proliferation of multinucleated giant (globoid) cells and white matter demyelination.[218,220] Most patients (>85%) with Krabbe disease present in infancy, proceeding through 3 recognized stages: irritability, abnormal startle response, temperature dysregulation, and delayed/regressed development (stage I) proceeding to hypertonicity, myoclonus/seizure, and optic atrophy (stage II), then to a vegetative state (stage III).[221] A few patients presenting in childhood or adulthood have milder symptoms (paresis, ataxia, visual loss) with variable progression. Imaging findings are distinctive. On computed tomography, there is increased density in the thalami and more variably in the other deep gray nuclei and other structures of the brain, some of which seem to represent frank calcification.[217,222,223] As the classic presentation occurs at 4 to 6 months of age, affected structures are often normally unmyelinated, which makes it difficult to appreciate signal abnormality on MR imaging.[224] For this reason, some advocate use of quantitative diffusion tensor imaging analysis in early suspected cases.[225,226] However, diagnosis is usually possible through recognition of T2 hypointensity of the thalami and unusual T2 prolongation in the dentate hila, posterior limb of the internal capsules, and the brainstem corticospinal tracts.[217,227] With time, increasing periventricular/central cerebral white matter and cerebellar white matter signal abnormality becomes evident, the former typically involving the corpus callosum.[228] Additional distinctive features include enhancement and thickening of cauda equina nerve roots and the cranial nerves, particularly the optic nerves.[229–233] Typical features of infantile Krabbe are shown in **Fig. 21** and as with most leukodystrophies there is progression to atrophy with time.[224,227,234] Later presentation forms of Krabbe manifest as signal abnormality confined to the posterior periventricular white matter and corticospinal tracts, resembling MLD or adrenomyeloneuropathy.[227,235]

MSUD

MSUD is an autosomal recessive disorder resulting from deficiency in components of the mitochondrial apparatus responsible for processing branched-chain α-ketoacids, metabolites derived from branched amino acids (eg, leucine, valine, isoleucine): subunit E1α *BCKDHA* (19q13),[236] subunit E1α *BCKDHA* (6p21),[237] and subunit E2 *DBT* (1p21).[238,239] The classic form of MSUD presents in the immediate neonatal period with poor feeding, lethargy, apnea, cerebral edema, and coma with associated ketonuria and maple syrup odor from urine. The intermediate form presents in later infancy or childhood with developmental delay and failure to thrive, reflecting higher residual enzyme activity. However, classic and intermediate MSUD as well as apparently normal children with branched-chain ketoacid deficiency (intermittent MSUD) can all develop metabolic decompensation including cerebral edema and coma when under physiologic stress (eg, mild infection).[240] Subunit E3 deficiency caused by mutations in *DLD* (7q31) affects additional enzymatic pathways (ie, pyruvate dehydrogenase) causing more complex phenotypes that overlap with other mitochondrial disorders.[241,242] Although the mechanism of brain pathology is incompletely understood, histologic examination of brains of patients with MSUD demonstrates spongiform changes in areas of myelinated nervous tissue.[243] Therefore, abnormal T2 signals in sites of neonatal brain myelination are present in classic MSUD including the posterior limb of the internal capsule as well as the dorsal brainstem, thalami, globus pallidus, and cerebellar white matter (**Fig. 22**)[244]; there are also reports of spinal cord involvement.[245] Intermediate MSUD may have an abnormal deep/periventricular white matter signal in addition to the typical brainstem sites in classic MSUD.[243,246,247] In acute decompensation, there is restricted diffusion in sites of signal abnormality, diffuse cerebral edema, and a characteristic MR spectroscopy peak at 0.9 ppm corresponding to branched-chain amino acid and α-ketoacid in addition to a lactate peak.[248–250] With supportive care and dietary restriction of leucine, there may be near resolution of signal abnormalities or mild residual T2 abnormality in sites of involvement with variable degrees of volume loss including prominent perivascular spaces.

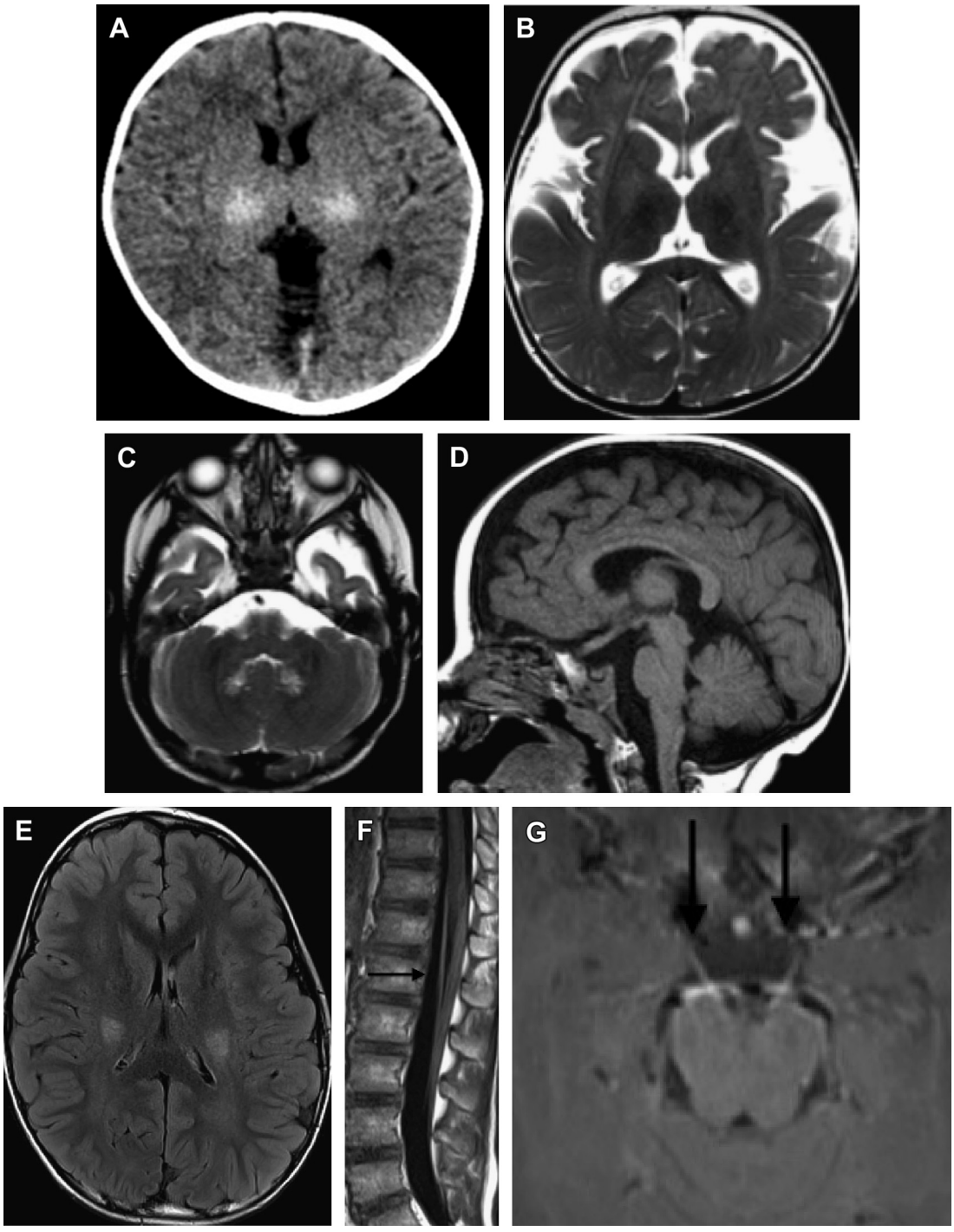

Fig. 21. Krabbe disease. Infantile presentation in 6-month-old children with increased irritability and extremity hypotonia: Axial computed tomography (*A*) demonstrates hyperdensity of the thalami. Axial T2-weighted images (*B, C*) demonstrate hypointensity of the thalamus as well as dentate nucleus signal increase and suggestion of corticospinal tract signal increase. Sagittal T1 (*D*) images demonstrate thickening of the optic nerves. Although the opercula are unusually prominent, the thickening of the optic nerves and the dense appearance of the thalamus suggested Krabbe rather than glutaric aciduria I, which was also considered. Juvenile presentation of Krabbe in a 6-year-old with motor regression: Axial Fluid attenuated inversion recovery images demonstrate signal increase in the corticospinal tracts (*E*). Postcontrast images demonstrate enhancement (*arrows*) of the cauda equina (*F*) and oculomotor nerves (*G*).

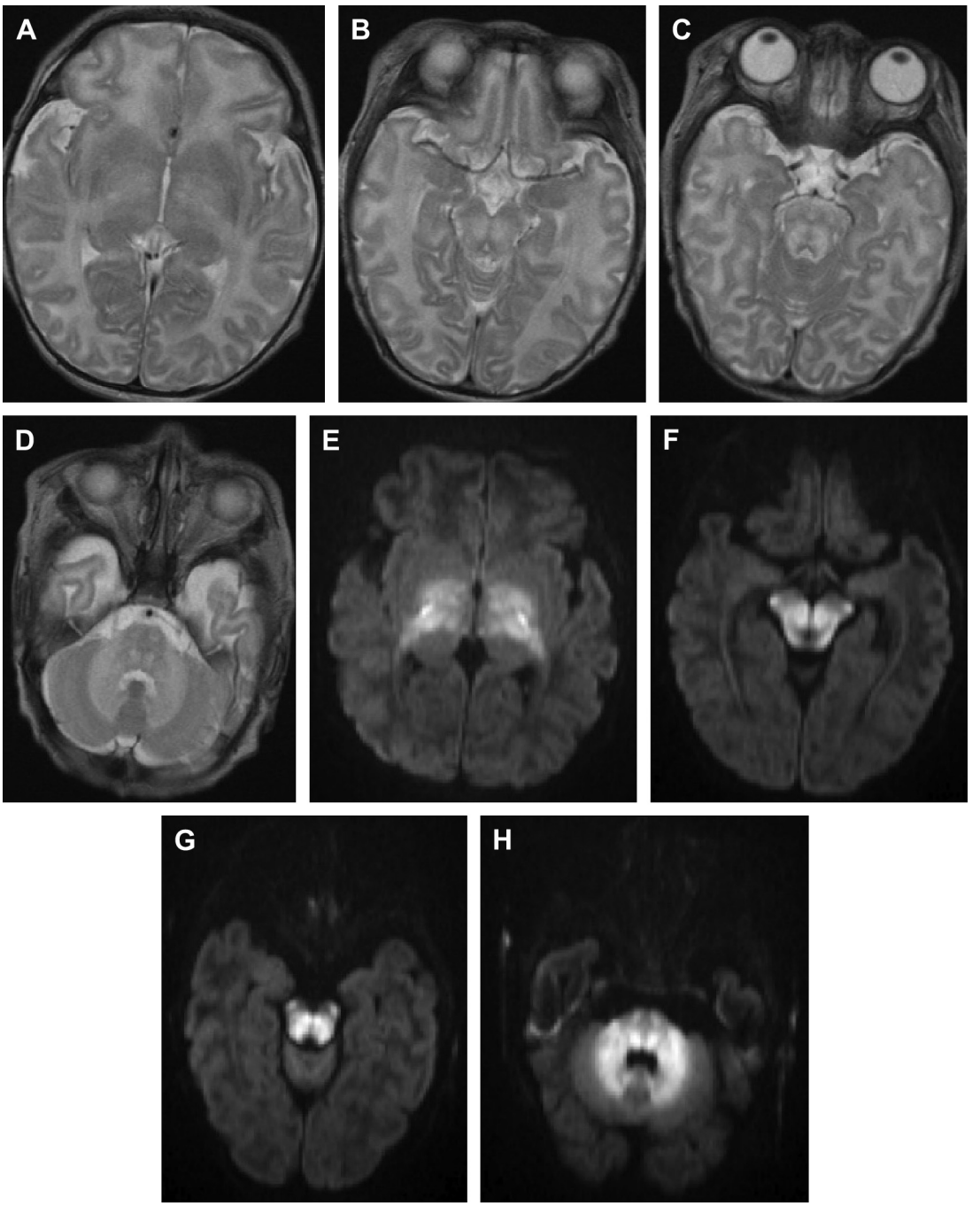

Fig. 22. Eleven-day-old infant with newly diagnosed maple syrup urine disease. Axial T2-weighted (*A–D*) and diffusion-weighted trace images (*E–H*) demonstrate signal abnormality and restricted diffusion in sites of normal neonatal brain myelination: posterior limbs of the internal capsule (*A, E*), brainstem corticospinal tracts (*B–D, F–H*), dorsal brainstem (*B, C, F, G*), and the cerebellar peduncles (*D, H*). The restricted diffusion is typical for patients imaged in acute decompensation.

Gray Matter Diseases with Some Extension into White Matter: Urea Cycle and Mitochondrial Disorders

Although outside the scope of this review, it is important to acknowledge that metabolic disorders primarily affecting gray matter may have resemblance to pattern 4 leukodystrophies (**Fig. 23**). In the case of urea cycle disorders (caused by recessive mutations in 1 of 6 gene products, the ornithine transcarbamylase gene being on the X chromosome[251]), the insular cortex and deep gray matter are involved similar to noninherited causes of hyperammonemia (ie, hepatic encephalopathy).[252–255] However, severe cases of urea cycle disorders can present with subcortical white matter edema near these locations or more generalized cerebral edema, often with accompanying restricted diffusion. MR spectroscopy can be of assistance in suggesting hyperammonemia because there is often an increase in glutamine/glutamate.[256] If mitochondrial disorders are defined as disorders of the oxidative phosphorylation pathway regardless of clinical syndrome (eg, Leigh syndrome; mitochondrial encephalomyopathy lactic acidosis, and strokelike episodes or MELAS), there is a strong predisposition for signal abnormalities of the deep gray

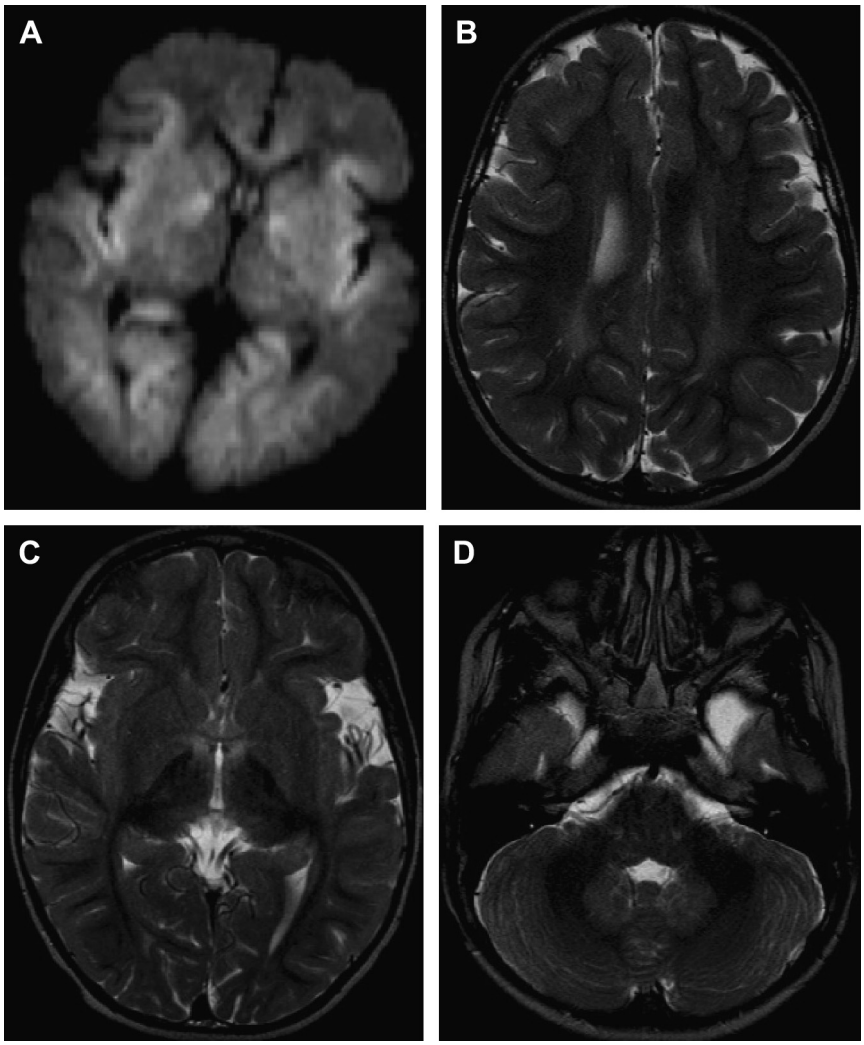

Fig. 23. Gray and white matter involvement in urea cycle and mitochondrial disorders. Six-day-old boy with ornithine transcarbamylase deficiency and seizure: diffusion-weighted image (*A*) demonstrates insular cortex and globus pallidus signal abnormality as well as areas of subcortical white matter hyperintensity. Three-year-old child with glutaric aciduria type I: axial T2-weighted images (*B–D*) demonstrate periventricular, basal ganglia, and dentate signal abnormality as well as the characteristic opercular widening seen in this disorder.

matter, brainstem (eg, central tegmental tracts), and (in the case of MELAS) cortical gray matter. However, there can also clearly be white matter involvement associated with these mitochondrial disorders resembling the leukodystrophies discussed in this review.[257] For mutations affecting complex I, white matter lesions were present in roughly a quarter of patients according to a recent review of the topic,[258,259] and for Kearns-Sayre syndrome (progressive external ophthalmoplegia, retinopathy), subcortical white matter signal abnormality usually accompanies the deep gray matter signal increase.[260] A high frequency of periventricular white matter signal abnormality in addition to deep gray signal increase and widened opercula are also seen in glutaric aciduria type I,[261] although this disorder (glutaryl dehydrogenase deficiency) is involved in mitochondrial amino acid catabolism not the respiratory chain directly. The relationships between genomic or mitochondrial DNA defects and specific imaging phenotypes are elusive at present, including for mitochondrial disorders with white matter manifestations.[262]

SUMMARY

As illustrated by the disease entities discussed in this article, leukodystrophies encompass a wide spectrum of imaging manifestations from delay in myelination to complex patterns of signal abnormality involving both white and gray matter. Although the diversity and number of diseases can seem overwhelming, imaging features allow separation of leukodystrophies into distinct categories, 4 of which have been emphasized in this review. With the addition of relevant clinical information and the presence of highly characteristic imaging findings (eg, parenchymal calcifications and photosensitivity in CS; macrocephaly and increased NAA in Canavan disease), a specific diagnosis can often be suggested. But even in cases where fairly generic findings are present (eg, delay in myelination), careful attention to the imaging patterns mentioned in this article can provide a small enough differential to guide an efficient workup. As historical testing strategies transition to an era of whole-genome sequencing, these imaging patterns can be expected to endure as a means of guiding interpretation of genetic data and potentially classifying new disorders.

REFERENCES

1. Seitelberger F. Structural manifestations of leukodystrophies. Neuropediatrics 1984;15(Suppl):53–61.
2. Menkes JH. The leukodystrophies. N Engl J Med 1990;322(1):54–5.
3. van der Knaap M, Valk J. Classification of myelin disorders. Magnetic resonance of myelination and myelin disorders. Berlin: Springer-Verlag; 2005.
4. Leite CC, Lucato LT, Martin MG, et al. Merosin-deficient congenital muscular dystrophy (CMD): a study of 25 Brazilian patients using MRI. Pediatr Radiol 2005;35(6):572–9.
5. Mercuri E, Topaloglu H, Brockington M, et al. Spectrum of brain changes in patients with congenital muscular dystrophy and FKRP gene mutations. Arch Neurol 2006;63(2):251–7.
6. van der Knaap MS, Smit LM, Barth PG, et al. Magnetic resonance imaging in classification of congenital muscular dystrophies with brain abnormalities. Ann Neurol 1997;42(1):50–9.
7. Poll-The BT, Gartner J. Clinical diagnosis, biochemical findings and MRI spectrum of peroxisomal disorders. Biochim Biophys Acta 2012;1822(9):1421–9.
8. van der Knaap M, Valk J. Magnetic resonance of myelination and myelin disorders. Berlin: Springer-Verlag; 2005.
9. Patay Z. Metabolic disorders. In: Tortori-Donati P, editor. Pediatric neuroradiology, vol. 1. Berlin: Springer-Verlag; 2005. p. 543–721.
10. Barkovich AJ, Patay Z. Metabolic, toxic, and inflammatory brain disorders. In: Barkovich AJ, editor. Pediatric neuroimaging. Philadelphia: Lippincott Williams & Wilkins; 2012. p. 81–239.
11. Leijser LM, de Vries LS, Rutherford MA, et al. Cranial ultrasound in metabolic disorders presenting in the neonatal period: characteristic features and comparison with MR imaging. AJNR Am J Neuroradiol 2007;28(7):1223–31.
12. Patay Z. Diffusion-weighted MR imaging in leukodystrophies. Eur Radiol 2005;15(11):2284–303.
13. Melhem ER, Loes DJ, Georgiades CS, et al. X-linked adrenoleukodystrophy: the role of contrast-enhanced MR imaging in predicting disease progression. AJNR Am J Neuroradiol 2000;21(5):839–44.
14. Cecil KM. MR spectroscopy of metabolic disorders. Neuroimaging Clin N Am 2006;16(1):87–116, viii.
15. Cakmakci H, Pekcevik Y, Yis U, et al. Diagnostic value of proton MR spectroscopy and diffusion-weighted MR imaging in childhood inherited neurometabolic brain diseases and review of the literature. Eur J Radiol 2010;74(3):e161–71.
16. Lange T, Dydak U, Roberts TP, et al. Pitfalls in lactate measurements at 3T. AJNR Am J Neuroradiol 2006;27(4):895–901.
17. Afifi AK, Menezes AH, Reed LA, et al. Atypical presentation of X-linked childhood adrenoleukodystrophy with an unusual magnetic resonance imaging pattern. J Child Neurol 1996;11(6):497–9.

18. van der Knaap MS, Salomons GS, Li R, et al. Unusual variants of Alexander's disease. Ann Neurol 2005;57(3):327–38.
19. Barkovich AJ. Concepts of myelin and myelination in neuroradiology. AJNR Am J Neuroradiol 2000; 21(6):1099–109.
20. van der Knaap MS, Breiter SN, Naidu S, et al. Defining and categorizing leukoencephalopathies of unknown origin: MR imaging approach. Radiology 1999;213(1):121–33.
21. Bonkowsky JL, Nelson C, Kingston JL, et al. The burden of inherited leukodystrophies in children. Neurology 2010;75(8):718–25.
22. Vanderver A, Hussey H, Schmidt JL, et al. Relative incidence of inherited white matter disorders in childhood to acquired pediatric demyelinating disorders. Semin Pediatr Neurol 2012;19(4): 219–23.
23. Heim P, Claussen M, Hoffmann B, et al. Leukodystrophy incidence in Germany. Am J Med Genet 1997;71(4):475–8.
24. Kohlschutter A, Eichler F. Childhood leukodystrophies: a clinical perspective. Expert Rev Neurother 2011;11(10):1485–96.
25. Kaye CI, Committee on Genetics, Accurso F, et al. Introduction to the newborn screening fact sheets. Pediatrics 2006;118(3):1304–12.
26. Woodward KJ. The molecular and cellular defects underlying Pelizaeus-Merzbacher disease. Expert Rev Mol Med 2008;10:e14.
27. van der Knaap M, Valk J. Pelizaeus-Merzbacher disease and X-linked spastic paraplegia type 2. Magnetic resonance of myelination and myelin disorders. Berlin: Springer-Verlag; 2005.
28. Southwood CM, Garbern J, Jiang W, et al. The unfolded protein response modulates disease severity in Pelizaeus-Merzbacher disease. Neuron 2002;36(4):585–96.
29. Gow A, Lazzarini RA. A cellular mechanism governing the severity of Pelizaeus-Merzbacher disease. Nat Genet 1996;13(4):422–8.
30. Hobson GM, Garbern JY. Pelizaeus-Merzbacher disease, Pelizaeus-Merzbacher-like disease 1, and related hypomyelinating disorders. Semin Neurol 2012;32(1):62–7.
31. van der Knaap MS, Valk J. The reflection of histology in MR imaging of Pelizaeus-Merzbacher disease. AJNR Am J Neuroradiol 1989;10(1):99–103.
32. Linnankivi T, Tienari P, Somer M, et al. 18q deletions: clinical, molecular, and brain MRI findings of 14 individuals. Am J Med Genet A 2006; 140(4):331–9.
33. Feenstra I, Vissers LE, Orsel M, et al. Genotype-phenotype mapping of chromosome 18q deletions by high-resolution array CGH: an update of the phenotypic map. Am J Med Genet A 2007; 143A(16):1858–67.
34. Lancaster JL, Cody JD, Andrews T, et al. Myelination in children with partial deletions of chromosome 18q. AJNR Am J Neuroradiol 2005;26(3):447–54.
35. Linnankivi TT, Autti TH, Pihko SH, et al. 18q-syndrome: brain MRI shows poor differentiation of gray and white matter on T2-weighted images. J Magn Reson Imaging 2003;18(4):414–9.
36. Tanaka R, Iwasaki N, Hayashi M, et al. Abnormal brain MRI signal in 18q-syndrome not due to dysmyelination. Brain Dev 2012;34(3):234–7.
37. Verheijen FW, Verbeek E, Aula N, et al. A new gene, encoding an anion transporter, is mutated in sialic acid storage diseases. Nat Genet 1999;23(4): 462–5.
38. Adams D, Gahl WA. Free sialic acid storage disorders. GeneReviews 2008. Available at: http://www.ncbi.nlm.nih.gov/books/NBK1470/. Accessed April 2, 2013.
39. Leroy PL. Sialuria. GeneReviews 2012. Available at: http://www.ncbi.nlm.nih.gov/books/NBK1164/. Accessed April 2, 2013.
40. Sonninen P, Autti T, Varho T, et al. Brain involvement in Salla disease. AJNR Am J Neuroradiol 1999; 20(3):433–43.
41. Haataja L, Parkkola R, Sonninen P, et al. Phenotypic variation and magnetic resonance imaging (MRI) in Salla disease, a free sialic acid storage disorder. Neuropediatrics 1994;25(5):238–44.
42. Varho T, Komu M, Sonninen P, et al. A new metabolite contributing to N-acetyl signal in 1H MRS of the brain in Salla disease. Neurology 1999;52(8): 1668–72.
43. Mochel F, Yang B, Barritault J, et al. Free sialic acid storage disease without sialuria. Ann Neurol 2009; 65(6):753–7.
44. van der Knaap M, Valk J. Fucosidosis. Magnetic resonance of myelination and myelin disorders. Berlin: Springer-Verlag; 2005.
45. Steenweg ME, Vanderver A, Blaser S, et al. Magnetic resonance imaging pattern recognition in hypomyelinating disorders. Brain 2010;133(10): 2971–82.
46. Prietsch V, Arnold S, Kraegeloh-Mann I, et al. Severe hypomyelination as the leading neuroradiological sign in a patient with fucosidosis. Neuropediatrics 2008;39(1):51–4.
47. Oner AY, Cansu A, Akpek S, et al. Fucosidosis: MRI and MRS findings. Pediatr Radiol 2007;37(10): 1050–2.
48. Mamourian AC, Hopkin JR, Chawla S, et al. Characteristic MR spectroscopy in fucosidosis: in vitro investigation. Pediatr Radiol 2010;40(8):1446–9.
49. Uhlenberg B, Schuelke M, Ruschendorf F, et al. Mutations in the gene encoding gap junction protein alpha 12 (connexin 46.6) cause Pelizaeus-Merzbacher-like disease. Am J Hum Genet 2004; 75(2):251–60.

50. Bugiani M, Al Shahwan S, Lamantea E, et al. GJA12 mutations in children with recessive hypomyelinating leukoencephalopathy. Neurology 2006;67(2):273–9.
51. Magen D, Georgopoulos C, Bross P, et al. Mitochondrial hsp60 chaperonopathy causes an autosomal-recessive neurodegenerative disorder linked to brain hypomyelination and leukodystrophy. Am J Hum Genet 2008;83(1):30–42.
52. Vaurs-Barriere C, Deville M, Sarret C, et al. Pelizaeus-Merzbacher-Like disease presentation of MCT8 mutated male subjects. Ann Neurol 2009; 65(1):114–8.
53. Feinstein M, Markus B, Noyman I, et al. Pelizaeus-Merzbacher-like disease caused by AIMP1/p43 homozygous mutation. Am J Hum Genet 2010;87(6): 820–8.
54. Tetreault M, Choquet K, Orcesi S, et al. Recessive mutations in POLR3B, encoding the second largest subunit of Pol III, cause a rare hypomyelinating leukodystrophy. Am J Hum Genet 2011;89(5):652–5.
55. Bernard G, Chouery E, Putorti ML, et al. Mutations of POLR3A encoding a catalytic subunit of RNA polymerase Pol III cause a recessive hypomyelinating leukodystrophy. Am J Hum Genet 2011;89(3): 415–23.
56. Harreld JH, Smith EC, Prose NS, et al. Trichothiodystrophy with dysmyelination and central osteosclerosis. AJNR Am J Neuroradiol 2010;31(1): 129–30.
57. Zara F, Biancheri R, Bruno C, et al. Deficiency of hyccin, a newly identified membrane protein, causes hypomyelination and congenital cataract. Nat Genet 2006;38(10):1111–3.
58. van der Knaap MS, Naidu S, Pouwels PJ, et al. New syndrome characterized by hypomyelination with atrophy of the basal ganglia and cerebellum. AJNR Am J Neuroradiol 2002;23(9):1466–74.
59. Simons C, Wolf NI, McNeil N, et al. A de novo mutation in the beta-Tubulin gene TUBB4A results in the leukoencephalopathy hypomyelination with atrophy of the basal ganglia and cerebellum. Am J Hum Genet 2013;92(5):767–73.
60. Hamosh A, Scharer G, Van Hove J. Glycine encephalopathy. In: Pagon RA, Bird TD, Dolan CR, et al, editors. GeneReviews. Seattle (WA): 1993. Available at: http://www.ncbi.nlm.nih.gov/books/NBK1357/.
61. Mourmans J, Majoie CB, Barth PG, et al. Sequential MR imaging changes in nonketotic hyperglycinemia. AJNR Am J Neuroradiol 2006;27(1):208–11.
62. Khong PL, Lam BC, Chung BH, et al. Diffusion-weighted MR imaging in neonatal nonketotic hyperglycinemia. AJNR Am J Neuroradiol 2003;24(6): 1181–3.
63. Viola A, Chabrol B, Nicoli F, et al. Magnetic resonance spectroscopy study of glycine pathways in nonketotic hyperglycinemia. Pediatr Res 2002; 52(2):292–300.
64. Gabis L, Parton P, Roche P, et al. In vivo 1H magnetic resonance spectroscopic measurement of brain glycine levels in nonketotic hyperglycinemia. J Neuroimaging 2001;11(2):209–11.
65. Fridovich-Keil JL. Galactosemia: the good, the bad, and the unknown. J Cell Physiol 2006; 209(3):701–5.
66. Ridel KR, Leslie ND, Gilbert DL. An updated review of the long-term neurological effects of galactosemia. Pediatr Neurol 2005;33(3):153–61.
67. van der Knaap M, Valk J. Galactosemia. Magnetic resonance of myelination and myelin disorders. Berlin: Springer-Verlag; 2005.
68. Otaduy MC, Leite CC, Lacerda MT, et al. Proton MR spectroscopy and imaging of a galactosemic patient before and after dietary treatment. AJNR Am J Neuroradiol 2006;27(1):204–7.
69. Wang ZJ, Berry GT, Dreha SF, et al. Proton magnetic resonance spectroscopy of brain metabolites in galactosemia. Ann Neurol 2001;50(2):266–9.
70. Leegwater PA, Boor PK, Yuan BQ, et al. Identification of novel mutations in MLC1 responsible for megalencephalic leukoencephalopathy with subcortical cysts. Hum Genet 2002;110(3):279–83.
71. van der Knaap MS, Boor I, Estevez R. Megalencephalic leukoencephalopathy with subcortical cysts: chronic white matter oedema due to a defect in brain ion and water homoeostasis. Lancet Neurol 2012;11(11):973–85.
72. van der Knaap MS, Barth PG, Stroink H, et al. Leukoencephalopathy with swelling and a discrepantly mild clinical course in eight children. Ann Neurol 1995;37(3):324–34.
73. Lopez-Hernandez T, Ridder MC, Montolio M, et al. Mutant GlialCAM causes megalencephalic leukoencephalopathy with subcortical cysts, benign familial macrocephaly, and macrocephaly with retardation and autism. Am J Hum Genet 2011;88(4):422–32.
74. Aicardi J, Goutieres F. A progressive familial encephalopathy in infancy with calcifications of the basal ganglia and chronic cerebrospinal fluid lymphocytosis. Ann Neurol 1984;15(1):49–54.
75. Baraitser M, Brett EM, Piesowicz AT. Microcephaly and intracranial calcification in two brothers. J Med Genet 1983;20(3):210–2.
76. Aicardi J, Crow YJ, Stephenson J. Aicardi-Goutieres syndrome. GeneReviews 2012. Available at: http://www.ncbi.nlm.nih.gov/books/NBK1475/. Accessed April 3, 2013.
77. Crow YJ, Hayward BE, Parmar R, et al. Mutations in the gene encoding the 3'-5' DNA exonuclease TREX1 cause Aicardi-Goutieres syndrome at the AGS1 locus. Nat Genet 2006;38(8):917–20.
78. Crow YJ, Leitch A, Hayward BE, et al. Mutations in genes encoding ribonuclease H2 subunits cause

Aicardi-Goutieres syndrome and mimic congenital viral brain infection. Nat Genet 2006;38(8):910–6.
79. Rice GI, Bond J, Asipu A, et al. Mutations involved in Aicardi-Goutieres syndrome implicate SAMHD1 as regulator of the innate immune response. Nat Genet 2009;41(7):829–32.
80. Rice GI, Kasher PR, Forte GM, et al. Mutations in ADAR1 cause Aicardi-Goutieres syndrome associated with a type I interferon signature. Nat Genet 2012;44(11):1243–8.
81. Vogt J, Agrawal S, Ibrahim Z, et al. Striking intrafamilial phenotypic variability in Aicardi-Goutieres syndrome associated with the recurrent Asian founder mutation in RNASEH2C. Am J Med Genet A 2013;161A(2):338–42.
82. Rice G, Patrick T, Parmar R, et al. Clinical and molecular phenotype of Aicardi-Goutieres syndrome. Am J Hum Genet 2007;81(4):713–25.
83. Chahwan C, Chahwan R. Aicardi-Goutieres syndrome: from patients to genes and beyond. Clin Genet 2012;81(5):413–20.
84. Ravenscroft JC, Suri M, Rice GI, et al. Autosomal dominant inheritance of a heterozygous mutation in SAMHD1 causing familial chilblain lupus. Am J Med Genet A 2011;155A(1):235–7.
85. Rice G, Newman WG, Dean J, et al. Heterozygous mutations in TREX1 cause familial chilblain lupus and dominant Aicardi-Goutieres syndrome. Am J Hum Genet 2007;80(4):811–5.
86. Uggetti C, La Piana R, Orcesi S, et al. Aicardi-Goutieres syndrome: neuroradiologic findings and follow-up. AJNR Am J Neuroradiol 2009;30(10):1971–6.
87. Chen X, DeLellis RA, Hoda SA. Adrenoleukodystrophy. Arch Pathol Lab Med 2003;127(1):119–20.
88. Eichler FS, Ren JQ, Cossoy M, et al. Is microglial apoptosis an early pathogenic change in cerebral X-linked adrenoleukodystrophy? Ann Neurol 2008;63(6):729–42.
89. van der Knaap M, Valk J. X-linked adrenoleukodystrophy. Magnetic resonance of myelination and myelin disorders. Berlin: Springer-Verlag; 2005.
90. Steinberg SJ, Moser AB, Raymond GV. X-linked adrenoleukodystrophy. GeneReviews 2012. Available at: http://www.ncbi.nlm.nih.gov/books/NBK1315/. Accessed April 4, 2013.
91. Ito R, Melhem ER, Mori S, et al. Diffusion tensor brain MR imaging in X-linked cerebral adrenoleukodystrophy. Neurology 2001;56(4):544–7.
92. Carrozzo R, Bellini C, Lucioli S, et al. Peroxisomal acyl-CoA-oxidase deficiency: two new cases. Am J Med Genet A 2008;146A(13):1676–81.
93. van der Knaap MS, Wassmer E, Wolf NI, et al. MRI as diagnostic tool in early-onset peroxisomal disorders. Neurology 2012;78(17):1304–8.
94. Kumar AJ, Kohler W, Kruse B, et al. MR findings in adult-onset adrenoleukodystrophy. AJNR Am J Neuroradiol 1995;16(6):1227–37.
95. Dubey P, Fatemi A, Huang H, et al. Diffusion tensor-based imaging reveals occult abnormalities in adrenomyeloneuropathy. Ann Neurol 2005;58(5):758–66.
96. Loes DJ, Fatemi A, Melhem ER, et al. Analysis of MRI patterns aids prediction of progression in X-linked adrenoleukodystrophy. Neurology 2003;61(3):369–74.
97. Dekaban AS, Constantopoulos G. Mucopolysaccharidosis type I, II, IIIA and V. Pathological and biochemical abnormalities in the neural and mesenchymal elements of the brain. Acta Neuropathol 1977;39(1):1–7.
98. van der Knaap M, Valk J. Mucopolysaccharidoses. Magnetic resonance of myelination and myelin disorders. Berlin: Springer-Verlag; 2005.
99. Azevedo AC, Artigalas O, Vedolin L, et al. Brain magnetic resonance imaging findings in patients with mucopolysaccharidosis VI. J Inherit Metab Dis 2013;36(2):357–62.
100. Barone R, Nigro F, Triulzi F, et al. Clinical and neuroradiological follow-up in mucopolysaccharidosis type III (Sanfilippo syndrome). Neuropediatrics 1999;30(5):270–4.
101. Manara R, Priante E, Grimaldi M, et al. Brain and spine MRI features of Hunter disease: frequency, natural evolution and response to therapy. J Inherit Metab Dis 2011;34(3):763–80.
102. Matheus MG, Castillo M, Smith JK, et al. Brain MRI findings in patients with mucopolysaccharidosis types I and II and mild clinical presentation. Neuroradiology 2004;46(8):666–72.
103. Vedolin L, Schwartz IV, Komlos M, et al. Correlation of MR imaging and MR spectroscopy findings with cognitive impairment in mucopolysaccharidosis II. AJNR Am J Neuroradiol 2007;28(6):1029–33.
104. Wang RY, Cambray-Forker EJ, Ohanian K, et al. Treatment reduces or stabilizes brain imaging abnormalities in patients with MPS I and II. Mol Genet Metab 2009;98(4):406–11.
105. Fan Z, Styner M, Muenzer J, et al. Correlation of automated volumetric analysis of brain MR imaging with cognitive impairment in a natural history study of mucopolysaccharidosis II. AJNR Am J Neuroradiol 2010;31(7):1319–23.
106. Attree O, Olivos IM, Okabe I, et al. The Lowe's oculocerebrorenal syndrome gene encodes a protein highly homologous to inositol polyphosphate-5-phosphatase. Nature 1992;358(6383):239–42.
107. McPherson PS, Garcia EP, Slepnev VI, et al. A presynaptic inositol-5-phosphatase. Nature 1996;379(6563):353–7.
108. Lewis RA, Nussbaum RL, Brewer ED. Lowe syndrome. In: Pagon RA, Bird TD, Dolan CR, et al, editors. GeneReviews. Seattle (WA): 1993. Available at: http://www.ncbi.nlm.nih.gov/books/NBK1480/.

109. O'Tuama LA, Laster DW. Oculocerebrorenal syndrome: case report with CT and MR correlates. AJNR Am J Neuroradiol 1987;8(3):555–7.
110. Demmer LA, Wippold FJ 2nd, Dowton SB. Periventricular white matter cystic lesions in Lowe (oculocerebrorenal) syndrome. A new MR finding. Pediatr Radiol 1992;22(1):76–7.
111. Carroll WJ, Woodruff WW, Cadman TE. MR findings in oculocerebrorenal syndrome. AJNR Am J Neuroradiol 1993;14(2):449–51.
112. Schneider JF, Boltshauser E, Neuhaus TJ, et al. MRI and proton spectroscopy in Lowe syndrome. Neuropediatrics 2001;32(1):45–8.
113. Yuksel A, Karaca E, Albayram MS. Magnetic resonance imaging, magnetic resonance spectroscopy, and facial dysmorphism in a case of Lowe syndrome with novel OCRL1 gene mutation. J Child Neurol 2009;24(1):93–6.
114. Bergoffen J, Scherer SS, Wang S, et al. Connexin mutations in X-linked Charcot-Marie-Tooth disease. Science 1993;262(5142):2039–42.
115. Bird TD. Charcot-Marie-Tooth neuropathy X type 1. GeneReviews 2012. 2013. Available at: http://www.ncbi.nlm.nih.gov/pubmed/20301548. Accessed April 5, 2013.
116. Shy ME, Siskind C, Swan ER, et al. CMT1X phenotypes represent loss of GJB1 gene function. Neurology 2007;68(11):849–55.
117. Paulson HL, Garbern JY, Hoban TF, et al. Transient central nervous system white matter abnormality in X-linked Charcot-Marie-Tooth disease. Ann Neurol 2002;52(4):429–34.
118. Taylor RA, Simon EM, Marks HG, et al. The CNS phenotype of X-linked Charcot-Marie-Tooth disease: more than a peripheral problem. Neurology 2003;61(11):1475–8.
119. Hanemann CO, Bergmann C, Senderek J, et al. Transient, recurrent, white matter lesions in X-linked Charcot-Marie-Tooth disease with novel connexin 32 mutation. Arch Neurol 2003;60(4):605–9.
120. Laugel V. Cockayne syndrome: the expanding clinical and mutational spectrum. Mech Ageing Dev 2013;134(5–6):161–70.
121. Nance MA, Berry SA. Cockayne syndrome: review of 140 cases. Am J Med Genet 1992;42(1):68–84.
122. Koob M, Laugel V, Durand M, et al. Neuroimaging in Cockayne syndrome. AJNR Am J Neuroradiol 2010;31(9):1623–30.
123. Adachi M, Kawanami T, Ohshima F, et al. MR findings of cerebral white matter in Cockayne syndrome. Magn Reson Med Sci 2006;5(1):41–5.
124. van der Knaap M, Valk J. Cockayne syndrome. Magnetic resonance of myelination and myelin disorders. Berlin: Springer-Verlag; 2005.
125. van Berge L, Kevenaar J, Polder E, et al. Pathogenic mutations causing LBSL affect mitochondrial aspartyl-tRNA synthetase in diverse ways. Biochem J 2013;450(2):345–50.
126. Scheper GC, van der Klok T, van Andel RJ, et al. Mitochondrial aspartyl-tRNA synthetase deficiency causes leukoencephalopathy with brain stem and spinal cord involvement and lactate elevation. Nat Genet 2007;39(4):534–9.
127. van der Knaap MS, van der Voorn P, Barkhof F, et al. A new leukoencephalopathy with brainstem and spinal cord involvement and high lactate. Ann Neurol 2003;53(2):252–8.
128. van der Knaap M, Valk J. Leukoencephalopathy with brain stem and spinal cord involvement and elevated white matter lactate. Magnetic resonance of myelination and myelin disorders. Berlin: Springer-Verlag; 2005.
129. Steenweg ME, van Berge L, van Berkel CG, et al. Early-onset LBSL: how severe does it get? Neuropediatrics 2012;43(6):332–8.
130. Taft RJ, Vanderver A, Leventer RJ, et al. Mutations in DARS cause hypomyelination with brain stem and spinal cord involvement and leg spasticity. Am J Hum Genet 2013;92(5):774–80.
131. Fluharty AL. Arylsulfatase A deficiency. In: Pagon RA, Bird TD, Dolan CR, et al, editors. GeneReviews. Seattle (WA): 1993. Available at: http://www.ncbi.nlm.nih.gov/books/NBK1130/.
132. Al-Hassnan ZN, Al Dhalaan H, Patay Z, et al. Sphingolipid activator protein B deficiency: report of 9 Saudi patients and review of the literature. J Child Neurol 2009;24(12):1513–9.
133. Stevens RL, Fluharty AL, Kihara H, et al. Cerebroside sulfatase activator deficiency induced metachromatic leukodystrophy. Am J Hum Genet 1981;33(6):900–6.
134. Kihara H, Tsay KK, Fluharty AL. Genetic complementation in somatic cell hybrids of cerebroside sulfatase activator deficiency and metachromatic leukodystrophy fibroblasts. Hum Genet 1984;66(4):300–1.
135. MacFaul R, Cavanagh N, Lake BD, et al. Metachromatic leucodystrophy: review of 38 cases. Arch Dis Child 1982;57(3):168–75.
136. Polten A, Fluharty AL, Fluharty CB, et al. Molecular basis of different forms of metachromatic leukodystrophy. N Engl J Med 1991;324(1):18–22.
137. Groeschel S, Kehrer C, Engel C, et al. Metachromatic leukodystrophy: natural course of cerebral MRI changes in relation to clinical course. J Inherit Metab Dis 2011;34(5):1095–102.
138. Eichler F, Grodd W, Grant E, et al. Metachromatic leukodystrophy: a scoring system for brain MR imaging observations. AJNR Am J Neuroradiol 2009;30(10):1893–7.
139. Maia AC Jr, da Rocha AJ, da Silva CJ, et al. Multiple cranial nerve enhancement: a new MR imaging

finding in metachromatic leukodystrophy. AJNR Am J Neuroradiol 2007;28(6):999.
140. Faerber EN, Melvin J, Smergel EM. MRI appearances of metachromatic leukodystrophy. Pediatr Radiol 1999;29(9):669–72.
141. Caro PA, Marks HG. Magnetic resonance imaging and computed tomography in Pelizaeus-Merzbacher disease. Magn Reson Imaging 1990;8(6):791–6.
142. Dziewas R, Stogbauer F, Oelerich M, et al. A case of adrenomyeloneuropathy with unusual lesion pattern in magnetic resonance imaging. J Neurol 2001;248(4):341–2.
143. Nishio H, Kodama S, Matsuo T, et al. Cockayne syndrome: magnetic resonance images of the brain in a severe form with early onset. J Inherit Metab Dis 1988;11(1):88–102.
144. van der Voorn JP, Pouwels PJ, Kamphorst W, et al. Histopathologic correlates of radial stripes on MR images in lysosomal storage disorders. AJNR Am J Neuroradiol 2005;26(3):442–6.
145. Onur MR, Senol U, Mihci E, et al. Tigroid pattern on magnetic resonance imaging in Lowe syndrome. J Clin Neurosci 2009;16(1):112–4.
146. Cleary MA, Walter JH, Wraith JE, et al. Magnetic resonance imaging of the brain in phenylketonuria. Lancet 1994;344(8915):87–90.
147. Leuzzi V, Tosetti M, Montanaro D, et al. The pathogenesis of the white matter abnormalities in phenylketonuria. A multimodal 3.0 tesla MRI and magnetic resonance spectroscopy (1H MRS) study. J Inherit Metab Dis 2007;30(2): 209–16.
148. Willemsen MA, Van Der Graaf M, Van Der Knaap MS, et al. MR imaging and proton MR spectroscopic studies in Sjogren-Larsson syndrome: characterization of the leukoencephalopathy. AJNR Am J Neuroradiol 2004;25(4):649–57.
149. van der Knaap M, Valk J. Hyperhomocysteinemias. Magnetic resonance of myelination and myelin disorders. Berlin: Springer-Verlag; 2005.
150. Wilcken B. Leukoencephalopathies associated with disorders of cobalamin and folate metabolism. Semin Neurol 2012;32(1):68–74.
151. Mano T, Ono J, Kaminaga T, et al. Proton MR spectroscopy of Sjogren-Larsson's syndrome. AJNR Am J Neuroradiol 1999;20(9):1671–3.
152. Striano P, Specchio N, Biancheri R, et al. Clinical and electrophysiological features of epilepsy in Italian patients with CLN8 mutations. Epilepsy Behav 2007;10(1):187–91.
153. van der Knaap M, Valk J. Neuronal ceroid lipofuscinoses. Magnetic resonance of myelination and myelin disorders. Berlin: Springer-Verlag; 2005.
154. van der Knaap MS, Pronk JC, Scheper GC. Vanishing white matter disease. Lancet Neurol 2006;5(5): 413–23.
155. Leegwater PA, Vermeulen G, Konst AA, et al. Subunits of the translation initiation factor eIF2B are mutant in leukoencephalopathy with vanishing white matter. Nat Genet 2001;29(4):383–8.
156. van der Lei HD, Steenweg ME, Barkhof F, et al. Characteristics of early MRI in children and adolescents with vanishing white matter. Neuropediatrics 2012;43(1):22–6.
157. Kaul R, Gao GP, Aloya M, et al. Canavan disease: mutations among Jewish and non-Jewish patients. Am J Hum Genet 1994;55(1):34–41.
158. Kaul R, Gao GP, Balamurugan K, et al. Cloning of the human aspartoacylase cDNA and a common missense mutation in Canavan disease. Nat Genet 1993;5(2):118–23.
159. Matalon R, Michals K, Sebesta D, et al. Aspartoacylase deficiency and N-acetylaspartic aciduria in patients with Canavan disease. Am J Med Genet 1988;29(2):463–71.
160. Baslow MH. Brain N-acetylaspartate as a molecular water pump and its role in the etiology of Canavan disease: a mechanistic explanation. J Mol Neurosci 2003;21(3):185–90.
161. Matalon RM, Michals-Matalon K. Spongy degeneration of the brain, Canavan disease: biochemical and molecular findings. Front Biosci 2000;5: D307–11.
162. Namboodiri AM, Moffett JR, Arun P, et al. Defective myelin lipid synthesis as a pathogenic mechanism of Canavan disease. Adv Exp Med Biol 2006;576: 145–63 [discussion 361–3].
163. van der Knaap M, Valk J. Canavan disease. Magnetic resonance of myelination and myelin disorders. Berlin: Springer-Verlag; 2005.
164. Brismar J, Brismar G, Gascon G, et al. Canavan disease: CT and MR imaging of the brain. AJNR Am J Neuroradiol 1990;11(4):805–10.
165. McAdams HP, Geyer CA, Done SL, et al. CT and MR imaging of Canavan disease. AJNR Am J Neuroradiol 1990;11(2):397–9.
166. Toft PB, Geiss-Holtorff R, Rolland MO, et al. Magnetic resonance imaging in juvenile Canavan disease. Eur J Pediatr 1993;152(9):750–3.
167. Yalcinkaya C, Benbir G, Salomons GS, et al. Atypical MRI findings in Canavan disease: a patient with a mild course. Neuropediatrics 2005;36(5):336–9.
168. Zafeiriou DI, Kleijer WJ, Maroupoulos G, et al. Protracted course of N-acetylaspartic aciduria in two non-Jewish siblings: identical clinical and magnetic resonance imaging findings. Brain Dev 1999;21(3):205–8.
169. Grodd W, Krageloh-Mann I, Klose U, et al. Metabolic and destructive brain disorders in children: findings with localized proton MR spectroscopy. Radiology 1991;181(1):173–81.
170. Janson CG, McPhee SW, Francis J, et al. Natural history of Canavan disease revealed by proton

magnetic resonance spectroscopy (1H-MRS) and diffusion-weighted MRI. Neuropediatrics 2006; 37(4):209–21.
171. Rzem R, Veiga-da-Cunha M, Noel G, et al. A gene encoding a putative FAD-dependent L-2-hydroxyglutarate dehydrogenase is mutated in L-2-hydroxyglutaric aciduria. Proc Natl Acad Sci U S A 2004; 101(48):16849–54.
172. Kranendijk M, Struys EA, Salomons GS, et al. Progress in understanding 2-hydroxyglutaric acidurias. J Inherit Metab Dis 2012;35(4):571–87.
173. Steenweg ME, Salomons GS, Yapici Z, et al. L-2-Hydroxyglutaric aciduria: pattern of MR imaging abnormalities in 56 patients. Radiology 2009; 251(3):856–65.
174. Topcu M, Erdem G, Saatci I, et al. Clinical and magnetic resonance imaging features of L-2-hydroxyglutaric acidemia: report of three cases in comparison with Canavan disease. J Child Neurol 1996;11(5):373–7.
175. Patay Z, Mills JC, Lobel U, et al. Cerebral neoplasms in L-2 hydroxyglutaric aciduria: 3 new cases and meta-analysis of literature data. AJNR Am J Neuroradiol 2012;33(5):940–3.
176. Ye D, Ma S, Xiong Y, et al. R-2-Hydroxyglutarate as the key effector of IDH mutations promoting oncogenesis. Cancer Cell 2013;23(3):274–6.
177. Losman JA, Looper RE, Koivunen P, et al. (R)-2-hydroxyglutarate is sufficient to promote leukemogenesis and its effects are reversible. Science 2013;339(6127):1621–5.
178. van der Knaap MS, Jakobs C, Hoffmann GF, et al. D-2-hydroxyglutaric aciduria: further clinical delineation. J Inherit Metab Dis 1999;22(4): 404–13.
179. Choi C, Ganji SK, DeBerardinis RJ, et al. 2-hydroxyglutarate detection by magnetic resonance spectroscopy in IDH-mutated patients with gliomas. Nat Med 2012;18(4):624–9.
180. Pope WB, Prins RM, Albert Thomas M, et al. Non-invasive detection of 2-hydroxyglutarate and other metabolites in IDH1 mutant glioma patients using magnetic resonance spectroscopy. J Neurooncol 2012;107(1):197–205.
181. Brenner M, Johnson AB, Boespflug-Tanguy O, et al. Mutations in GFAP, encoding glial fibrillary acidic protein, are associated with Alexander disease. Nat Genet 2001;27(1):117–20.
182. Li R, Johnson AB, Salomons G, et al. Glial fibrillary acidic protein mutations in infantile, juvenile, and adult forms of Alexander disease. Ann Neurol 2005;57(3):310–26.
183. Messing A, Li R, Naidu S, et al. Archetypal and new families with Alexander disease and novel mutations in GFAP. Arch Neurol 2012;69(2):208–14.
184. Hagemann TL, Connor JX, Messing A. Alexander disease-associated glial fibrillary acidic protein mutations in mice induce Rosenthal fiber formation and a white matter stress response. J Neurosci 2006;26(43):11162–73.
185. Hsiao VC, Tian R, Long H, et al. Alexander-disease mutation of GFAP causes filament disorganization and decreased solubility of GFAP. J Cell Sci 2005;118(Pt 9):2057–65.
186. Messing A, Brenner M, Feany MB, et al. Alexander disease. J Neurosci 2012;32(15):5017–23.
187. Gorospe JR. Alexander disease. In: Pagon RA, Bird TD, Dolan CR, et al, editors. GeneReviews. Seattle (WA): 1993. Available at: http://www.ncbi.nlm.nih.gov/books/NBK1172/.
188. van der Knaap M, Valk J. GM1 gangliosidosis and GM2 gangliosidosis. Magnetic resonance of myelination and myelin disorders. Berlin: Springer-Verlag; 2005.
189. van der Knaap MS, Naidu S, Breiter SN, et al. Alexander disease: diagnosis with MR imaging. AJNR Am J Neuroradiol 2001;22(3):541–52.
190. van der Knaap MS, Ramesh V, Schiffmann R, et al. Alexander disease: ventricular garlands and abnormalities of the medulla and spinal cord. Neurology 2006;66(4):494–8.
191. Pareyson D, Fancellu R, Mariotti C, et al. Adult-onset Alexander disease: a series of eleven unrelated cases with review of the literature. Brain 2008;131(Pt 9):2321–31.
192. Stumpf E, Masson H, Duquette A, et al. Adult Alexander disease with autosomal dominant transmission: a distinct entity caused by mutation in the glial fibrillary acid protein gene. Arch Neurol 2003; 60(9):1307–12.
193. Jeyakumar M, Butters TD, Dwek RA, et al. Glycosphingolipid lysosomal storage diseases: therapy and pathogenesis. Neuropathol Appl Neurobiol 2002;28(5):343–57.
194. Okada S, O'Brien JS. Generalized gangliosidosis: beta-galactosidase deficiency. Science 1968; 160(3831):1002–4.
195. Nishimoto J, Nanba E, Inui K, et al. GM1-gangliosidosis (genetic beta-galactosidase deficiency): identification of four mutations in different clinical phenotypes among Japanese patients. Am J Hum Genet 1991;49(3):566–74.
196. Yoshida K, Oshima A, Shimmoto M, et al. Human beta-galactosidase gene mutations in GM1-gangliosidosis: a common mutation among Japanese adult/chronic cases. Am J Hum Genet 1991; 49(2):435–42.
197. Okada S, O'Brien JS. Tay-Sachs disease: generalized absence of a beta-D-N-acetylhexosaminidase component. Science 1969;165(3894):698–700.
198. Lalley PA, Rattazzi MC, Shows TB. Human beta-D-N-acetylhexosaminidases A and B: expression and linkage relationships in somatic cell hybrids. Proc Natl Acad Sci U S A 1974;71(4):1569–73.

199. Myerowitz R, Costigan FC. The major defect in Ashkenazi Jews with Tay-Sachs disease is an insertion in the gene for the alpha-chain of beta-hexosaminidase. J Biol Chem 1988;263(35):18587–9.
200. O'Dowd BF, Klavins MH, Willard HF, et al. Molecular heterogeneity in the infantile and juvenile forms of Sandhoff disease (O-variant GM2 gangliosidosis). J Biol Chem 1986;261(27):12680–5.
201. Gilbert F, Kucherlapati R, Creagan RP, et al. Tay-Sachs' and Sandhoff's diseases: the assignment of genes for hexosaminidase A and B to individual human chromosomes. Proc Natl Acad Sci U S A 1975;72(1):263–7.
202. Sandhoff K, Conzelmann E, Nehrkorn H. Substrate specificity of hexosaminidase A isolated from the liver of a patient with a rare form (AB variant) of infantile GM2 gangliosidosis and control tissues. Adv Exp Med Biol 1978;101:727–30.
203. Chen B, Rigat B, Curry C, et al. Structure of the GM2A gene: identification of an exon 2 nonsense mutation and a naturally occurring transcript with an in-frame deletion of exon 2. Am J Hum Genet 1999;65(1):77–87.
204. Brunetti-Pierri N, Scaglia F. GM1 gangliosidosis: review of clinical, molecular, and therapeutic aspects. Mol Genet Metab 2008;94(4):391–6.
205. Kaback MM, Desnick RJ. Hexosaminidase A deficiency. GeneReviews 1993. 2013. Available at: http://www.ncbi.nlm.nih.gov/pubmed/20301397. Accessed April 21, 2013.
206. Bley AE, Giannikopoulos OA, Hayden D, et al. Natural history of infantile G(M2) gangliosidosis. Pediatrics 2011;128(5):e1233–41.
207. Maegawa GH, Stockley T, Tropak M, et al. The natural history of juvenile or subacute GM2 gangliosidosis: 21 new cases and literature review of 134 previously reported. Pediatrics 2006;118(5):e1550–62.
208. Frey LC, Ringel SP, Filley CM. The natural history of cognitive dysfunction in late-onset GM2 gangliosidosis. Arch Neurol 2005;62(6):989–94.
209. Erol I, Alehan F, Pourbagher MA, et al. Neuroimaging findings in infantile GM1 gangliosidosis. Eur J Paediatr Neurol 2006;10(5–6):245–8.
210. Chen CY, Zimmerman RA, Lee CC, et al. Neuroimaging findings in late infantile GM1 gangliosidosis. AJNR Am J Neuroradiol 1998;19(9):1628–30.
211. Imamura A, Miyajima H, Ito R, et al. Serial MR imaging and 1H-MR spectroscopy in monozygotic twins with Tay-Sachs disease. Neuropediatrics 2008;39(5):259–63.
212. Inglese M, Nusbaum AO, Pastores GM, et al. MR imaging and proton spectroscopy of neuronal injury in late-onset GM2 gangliosidosis. AJNR Am J Neuroradiol 2005;26(8):2037–42.
213. Streifler JY, Gornish M, Hadar H, et al. Brain imaging in late-onset GM2 gangliosidosis. Neurology 1993;43(10):2055–8.
214. Uyama E, Terasaki T, Watanabe S, et al. Type 3 GM1 gangliosidosis: characteristic MRI findings correlated with dystonia. Acta Neurol Scand 1992;86(6):609–15.
215. Roze E, Paschke E, Lopez N, et al. Dystonia and parkinsonism in GM1 type 3 gangliosidosis. Mov Disord 2005;20(10):1366–9.
216. De Grandis E, Di Rocco M, Pessagno A, et al. MR imaging findings in 2 cases of late infantile GM1 gangliosidosis. AJNR Am J Neuroradiol 2009;30(7):1325–7.
217. van der Knaap M, Valk J. Globoid cell leukodystrophy: Krabbe disease. Magnetic resonance of myelination and myelin disorders. Berlin: Springer-Verlag; 2005.
218. Suzuki K, Suzuki Y. Globoid cell leucodystrophy (Krabbe's disease): deficiency of galactocerebroside beta-galactosidase. Proc Natl Acad Sci U S A 1970;66(2):302–9.
219. Spiegel R, Bach G, Sury V, et al. A mutation in the saposin A coding region of the prosaposin gene in an infant presenting as Krabbe disease: first report of saposin A deficiency in humans. Mol Genet Metab 2005;84(2):160–6.
220. Svennerholm L, Vanier MT, Mansson JE. Krabbe disease: a galactosylsphingosine (psychosine) lipidosis. J Lipid Res 1980;21(1):53–64.
221. Wenger DA. Krabbe disease. GeneReviews. 2013. Available at: http://www.ncbi.nlm.nih.gov/pubmed/20301416. Accessed April 25, 2013.
222. Choi S, Enzmann DR. Infantile Krabbe disease: complementary CT and MR findings. AJNR Am J Neuroradiol 1993;14(5):1164–6.
223. Livingston JH, Graziano C, Pysden K, et al. Intracranial calcification in early infantile Krabbe disease: nothing new under the sun. Dev Med Child Neurol 2012;54(4):376–9.
224. Finelli DA, Tarr RW, Sawyer RN, et al. Deceptively normal MR in early infantile Krabbe disease. AJNR Am J Neuroradiol 1994;15(1):167–71.
225. Escolar ML, Poe MD, Smith JK, et al. Diffusion tensor imaging detects abnormalities in the corticospinal tracts of neonates with infantile Krabbe disease. AJNR Am J Neuroradiol 2009;30(5):1017–21.
226. Guo AC, Petrella JR, Kurtzberg J, et al. Evaluation of white matter anisotropy in Krabbe disease with diffusion tensor MR imaging: initial experience. Radiology 2001;218(3):809–15.
227. Loes DJ, Peters C, Krivit W. Globoid cell leukodystrophy: distinguishing early-onset from late-onset disease using a brain MR imaging scoring method. AJNR Am J Neuroradiol 1999;20(2):316–23.
228. Sasaki M, Sakuragawa N, Takashima S, et al. MRI and CT findings in Krabbe disease. Pediatr Neurol 1991;7(4):283–8.

229. Bernal OG, Lenn N. Multiple cranial nerve enhancement in early infantile Krabbe's disease. Neurology 2000;54(12):2348–9.
230. Jones BV, Barron TF, Towfighi J. Optic nerve enlargement in Krabbe's disease. AJNR Am J Neuroradiol 1999;20(7):1228–31.
231. Morana G, Biancheri R, Dirocco M, et al. Enhancing cranial nerves and cauda equina: an emerging magnetic resonance imaging pattern in metachromatic leukodystrophy and krabbe disease. Neuropediatrics 2009;40(6):291–4.
232. Nagar VA, Ursekar MA, Krishnan P, et al. Krabbe disease: unusual MRI findings. Pediatr Radiol 2006;36(1):61–4.
233. Vasconcellos E, Smith M. MRI nerve root enhancement in Krabbe disease. Pediatr Neurol 1998; 19(2):151–2.
234. Zafeiriou DI, Michelakaki EM, Anastasiou AL, et al. Serial MRI and neurophysiological studies in late-infantile Krabbe disease. Pediatr Neurol 1996; 15(3):240–4.
235. Farina L, Bizzi A, Finocchiaro G, et al. MR imaging and proton MR spectroscopy in adult Krabbe disease. AJNR Am J Neuroradiol 2000;21(8):1478–82.
236. Zhang B, Zhao Y, Harris RA, et al. Molecular defects in the E1 alpha subunit of the branched-chain alpha-ketoacid dehydrogenase complex that cause maple syrup urine disease. Mol Biol Med 1991;8(1):39–47.
237. Nobukuni Y, Mitsubuchi H, Akaboshi I, et al. Maple syrup urine disease. Complete defect of the E1 beta subunit of the branched chain alpha-ketoacid dehydrogenase complex due to a deletion of an 11-bp repeat sequence which encodes a mitochondrial targeting leader peptide in a family with the disease. J Clin Invest 1991;87(5):1862–6.
238. Fisher CW, Lau KS, Fisher CR, et al. A 17-bp insertion and a Phe215–Cys missense mutation in the dihydrolipoyl transacylase (E2) mRNA from a thiamine-responsive maple syrup urine disease patient WG-34. Biochem Biophys Res Commun 1991; 174(2):804–9.
239. Herring WJ, Litwer S, Weber JL, et al. Molecular genetic basis of maple syrup urine disease in a family with two defective alleles for branched chain acyltransferase and localization of the gene to human chromosome 1. Am J Hum Genet 1991; 48(2):342–50.
240. Strauss KA, Puffenberger EG, Morton DH. Maple syrup urine disease. GeneReviews. 2013. Available at: http://www.ncbi.nlm.nih.gov/pubmed/20301495. Accessed April 26, 2013.
241. Shaag A, Saada A, Berger I, et al. Molecular basis of lipoamide dehydrogenase deficiency in Ashkenazi Jews. Am J Med Genet 1999;82(2):177–82.
242. Liu TC, Kim H, Arizmendi C, et al. Identification of two missense mutations in a dihydrolipoamide dehydrogenase-deficient patient. Proc Natl Acad Sci U S A 1993;90(11):5186–90.
243. van der Knaap M, Valk J. Maple syrup urine disease. Magnetic resonance of myelination and myelin disorders. Berlin: Springer-Verlag; 2005.
244. Brismar J, Aqeel A, Brismar G, et al. Maple syrup urine disease: findings on CT and MR scans of the brain in 10 infants. AJNR Am J Neuroradiol 1990;11(6):1219–28.
245. Bhat M, Prasad C, Bindu PS, et al. Unusual imaging findings in brain and spinal cord in two siblings with maple syrup urine disease. J Neuroimaging 2013;23(4):540–2.
246. Bindu PS, Shehanaz KE, Christopher R, et al. Intermediate maple syrup urine disease: neuroimaging observations in 3 patients from South India. J Child Neurol 2007;22(7):911–3.
247. Sener RN. Diffusion magnetic resonance imaging in intermediate form of maple syrup urine disease. J Neuroimaging 2002;12(4):368–70.
248. Cavalleri F, Berardi A, Burlina AB, et al. Diffusion-weighted MRI of maple syrup urine disease encephalopathy. Neuroradiology 2002;44(6):499–502.
249. Felber SR, Sperl W, Chemelli A, et al. Maple syrup urine disease: metabolic decompensation monitored by proton magnetic resonance imaging and spectroscopy. Ann Neurol 1993;33(4):396–401.
250. Jan W, Zimmerman RA, Wang ZJ, et al. MR diffusion imaging and MR spectroscopy of maple syrup urine disease during acute metabolic decompensation. Neuroradiology 2003;45(6):393–9.
251. Lanpher BC, Gropman A, Chapman KA, et al. Urea Cycle Disorders Consortium. Urea cycle disorders overview. GeneReviews. 2013. Available at: http://www.ncbi.nlm.nih.gov/pubmed/20301396. Accessed April 30, 2013.
252. Takanashi J, Barkovich AJ, Cheng SF, et al. Brain MR imaging in neonatal hyperammonemic encephalopathy resulting from proximal urea cycle disorders. AJNR Am J Neuroradiol 2003;24(6):1184–7.
253. Majoie CB, Mourmans JM, Akkerman EM, et al. Neonatal citrullinemia: comparison of conventional MR, diffusion-weighted, and diffusion tensor findings. AJNR Am J Neuroradiol 2004;25(1):32–5.
254. McKinney AM, Lohman BD, Sarikaya B, et al. Acute hepatic encephalopathy: diffusion-weighted and fluid-attenuated inversion recovery findings, and correlation with plasma ammonia level and clinical outcome. AJNR Am J Neuroradiol 2010;31(8): 1471–9.
255. Poveda MJ, Bernabeu A, Concepcion L, et al. Brain edema dynamics in patients with overt hepatic encephalopathy A magnetic resonance imaging study. Neuroimage 2010;52(2):481–7.
256. Choi CG, Yoo HW. Localized proton MR spectroscopy in infants with urea cycle defect. AJNR Am J Neuroradiol 2001;22(5):834–7.

257. Finsterer J, Jarius C, Eichberger H. Phenotype variability in 130 adult patients with respiratory chain disorders. J Inherit Metab Dis 2001;24(5):560–76.
258. Koene S, Rodenburg RJ, van der Knaap MS, et al. Natural disease course and genotype-phenotype correlations in Complex I deficiency caused by nuclear gene defects: what we learned from 130 cases. J Inherit Metab Dis 2012;35(5):737–47.
259. Sofou K, Steneryd K, Wiklund LM, et al. MRI of the brain in childhood-onset mitochondrial disorders with central nervous system involvement. Mitochondrion 2013;13(4):364–71.
260. Chu BC, Terae S, Takahashi C, et al. MRI of the brain in the Kearns-Sayre syndrome: report of four cases and a review. Neuroradiology 1999; 41(10):759–64.
261. Twomey EL, Naughten ER, Donoghue VB, et al. Neuroimaging findings in glutaric aciduria type 1. Pediatr Radiol 2003;33(12):823–30.
262. Morava E, Smeitink JA. Mitochondria and mitochondrial disorders. In: van der Knaap M, Valk J, editors. Magnetic resonance of myelination and myelin disorders. Berlin: Springer-Verlag; 2005. p. 195–203.